SLAC-PUB-1278
(T)
July 1973

QUANTUM ELECTRODYNAMICS AND RENORMALIZATION THEORY IN THE INFINITE MOMENTUM FRAME*

Stanley J. Brodsky
Stanford Linear Accelerator Center
Stanford, California 94305

Ralph Roskies†**
Yale University
New Haven, Connecticut 06520

Roberto Suaya††
Stanford Linear Accelerator Center
Stanford, California 94305

ABSTRACT

Time-ordered perturbation theory evaluated in the infinite momentum reference frame of Weinberg is shown to be a viable calculational alternative to the usual Feynman graph procedure for quantum electrodynamics. We derive the rules of calculation at infinite momentum, and introduce a convenient method for automatically including z graphs (backward moving fermion contributions). We then develop techniques for implementing renormalization theory, and apply these to various examples. We show that the $P \to \infty$ limit is uniform for calculating renormalized amplitudes, but this is not true in evaluating the renormalization constants themselves. Our rules are then applied to calculate the electron anomalous moment through fourth order and a representative diagram in sixth order. It is shown that our techniques are competitive with the normal Feynman approach in practical calculations. Some implications of our results, and connections with the light cone quantization, are discussed.

* Work supported by the U. S. Atomic Energy Commission.
† Present address: University of Pittsburgh, Pittsburgh, Pa. 15260.
** Supported in part by the U. S. Atomic Energy Commission under Contract AT(11-1)-3075.
†† Present address: University of Buenos Aires, Argentina. Address after August 1: University of Illinois, Urbana, Illinois.

(Submitted to Phys. Rev.)

I. INTRODUCTION

Over the past few years it has been shown that the use of an "infinite momentum" Lorentz frame[1] has remarkable advantages for calculations in elementary particle physics and field theory, especially in the areas of current algebra sum rules,[2] parton models,[3,4] and eikonal scattering.[5,6] One important advantage is that it allows a straightforward application of the impulse and incoherence approximations familiar in nonrelativistic atomic and nuclear physics to relativistic field theory and bound state problems.

We shall show that infinite momentum frame methods are also competitive with the usual Feynman methods in quantum electrodynamics. Despite the passage of over two decades, the basic methods for calculations in QED have changed little since the development of the Feynman-Dyson-Schwinger rules. Although it is true that dispersion theory calculations of the lepton vertex -- dispersing either in the photon mass or sidewise in one fermion leg -- do provide such an alternate procedure; in fact, such calculations are much more arduous than the standard Feynman method, often involving extremely subtle and treacherous nonuniform infrared problems,[7] and only are applicable to the two and three point amplitudes. The time-ordered perturbation theory -- infinite-momentum-frame-method ($TOPTh_\infty$) to be described here retains the main advantages of the dispersion method since calculations involve physical on-mass shell intermediate states of fixed particle number, but because of the $P \to \infty$ limit, the complicated square-root structure of the phase-space integration is automatically linearized, and the analysis of infrared divergences is no more difficult than in the corresponding Feynman calculations.

The field-theoretic aspects of time-ordered perturbation theory in the $P \to \infty$ limit were first studied by Weinberg[1] in spinless theories. The development of the parton model[3] by Drell, Levy and Yan motivated the extension of Weinberg's work to spin $\frac{1}{2}$ theories.[4] Because of the equivalence of TOPTh_∞ with conventional field theory demonstrated here for quantum electrodynamics (and by simple extension to the supperrenormalizable ϕ^3 theory and the renormalizable $\bar{\psi}\gamma_5\psi\pi$ pseudoscalar theory), such parton model calculations can acquire a rigorous basis. The important qualification is the necessity to use covariant regularization rather than a simple transverse momentum cutoff procedure in order to avoid difficulties with gauge invariance and covariance.

The $P \to \infty$ limit became of even greater interest when its relation to light cone quantization was realized.[6] In fact, the standard rules of calculation are identical in the two theories. The z-graph contributions of the TOPTh_∞ correspond to seagull terms in the interaction using the light-cone quantization method. However, the development of the calculational rules directly from the standard theory with the $P \to \infty$ limit allows one to develop renormalization theory and avoids errors due to non-uniform convergence in the $P \to \infty$ limit. For example, we clarify the subtleties involved in the light cone calculation of the electron self-mass. Our results agree with the analysis of this problem by Bouchiat, et al.[8] Our techniques show how to calculate quantum electrodynamics on the light-cone in the Feynman gauge, rather than in the Coulomb gauge, and how to implement the renormalization procedure.

After the work in this paper was completed, there have appeared other, more formal, proofs of the equivalence between light cone and conventional QED.[9] The approaches are somewhat complementary. Whereas these works show formally that light-cone-formulated and conventional QED have the same renormalized S matrices, we show that the $P \to \infty$ limit of time-ordered perturbation theory does give the light cone formulated rules. Moreover, we use this formalism to perform actual higher order calculations.

The plan of this paper is as follows: In section II, we rederive the rules for calculating Time Ordered Perturbation Theory (TOPTh) in the infinite momentum frame, and present an automatic method for incorporating the contributing "z-graphs" of spinor theories. Then, even in spinor theories only intermediate states in which each particle has positive compoment of momentum along P survive in the $P \to \infty$ limit. Moreover, we show that a single spinor or trace calculation suffices for all time ordered graphs corresponding to the same Feynman graph.

The renormalization procedure for TOPTh_∞ is presented in section III. We show that the $P \to \infty$ limit is uniformly convergent with respect to the phase space integrations when calculating renormalized amplitudes with invariant regularization, although this is not true for the evaluation of the renormalization constants themselves. Vacuum polarization and the general problem of photon and fermion self-energy insertions in higher order graphs is discussed. Examples of vertex subgraph renormalization in the fourth order electron vertex are also discussed. This section also contains a proof of the Ward identity in the context of TOPTh_∞, and a heuristic proof of the renormalizability of QED in TOPTh_∞.

In section IV we discuss some details of the calculation of the fourth order and some pieces of the sixth order anomalous magnetic moment of the electron. The required phase space integrations over transverse and fractional longitudinal momenta are in general regular and smooth, and are often more readily integrable than the standard Feynman parametric form.

In the Appendix we discuss a method which, in some cases, provides a direct connection between the Feynman rules and those at infinite momentum. This method provides further insight into how our z graph rules arise. We also comment that the connection between the Feynman and TOPTh_∞ rules is not simple in all cases.

II. THE RULES

The S matrix is related to the invariant matrix element M by

$$S = 1 - (2\pi)^4 i\,\delta^{(4)}(P_{final} - P_{initial})\,M \prod_{\substack{\text{external}\\ \text{particles}}} N_i\,. \qquad (2.1)$$

where N_i is the normalization factor $\frac{1}{(2\pi)^{3/2}}\frac{1}{\sqrt{2E_i}}$ and E_i is the energy of the i^{th} external particle. We now write the rules for calculating the contributions to M in the interaction picture in TOPTh. For the moment we restrict ourselves to spinless particles with a ϕ^3 interaction. We first classify the time-ordered contributions according to their Feynman topologies. Then

1. For each Feynman graph of order n, assign a time t_i to the i^{th} vertex. Then draw n! graphs, corresponding to all permutations of the times t_i, with the same topology as the Feynman graph. As an example, to the simple Feynman vertex graph of Figure 1, there correspond six time-ordered graphs as shown in Figure 2. (By convention, time flows from left to right.)

2. With each line of each time ordered graph, associate a three-momentum.

3. At each vertex except the last, write a factor $(2\pi)^3 g\,\delta^{(3)}(\sum \vec{p_i})$ where g is the coupling constant, and the delta function expresses three-momentum conservation at that vertex. At the last vertex insert only a factor g, since the factor $(2\pi)^3\delta^{(3)}(\sum \vec{p_i})$ has already been taken out of M in (2.1).

4. For each internal line write a factor $\frac{1}{(2\pi)^3} \frac{1}{2E_i}$ where E_i is the energy of the line in question, calculated on the mass shell, i.e.,

$$E_i = \sqrt{\vec{p}_i^{\,2} + m_i^2} \tag{2.2}$$

5. For each intermediate state, i.e., for each state between interaction times, write a factor

$$\frac{1}{E_{inc} - E_{int} + i\epsilon}$$

where E_{inc} is the total energy of the incoming particles, and E_{int} is the energy of the intermediate state, obtained by adding the single particle energies of all particles in that particular state.

6. Integrate d^3p_i.

7. Add the contributions of all the different time ordered graphs.

One sees several features which distinguish TOPTh from the Feynman approach. First, every intermediate particle is on its mass shell, but energy is not conserved, while in the Feynman approach, energy is conserved but particles are off the mass shell. Second, all particles propagate forward in time, and the number of particles in a given intermediate state is clear. Third, manifest covariance is gone. One can summarize these last two points by saying that TOPTh emphasizes the unitarity of the theory, while the usual approach emphasizes its covariance. Fourth, there are many more graphs to calculate in TOPTh than in the Feynman approach.

Points three and four are usually considered serious practical shortcomings of TOPTh. However, Weinberg[1] realized that the lack of manifest covariance could be used to good advantage. He argued that since the sum of the time-ordered graphs was covariant, although each of the graphs by itself was not, it might be possible to find a frame of reference in which it was particularly simple to calculate each of these graphs. In particular, there might be a frame in which one could recognize immediately that most of the graphs gave a vanishing contribution. That frame is the infinite momentum frame.

Let us review his argument. We view the scattering process from a frame moving rapidly in the negative z direction, so that the total incident momentum $\vec{P}$ is large and along the positive z direction. We will show that as $P \to \infty$, each of the time ordered graphs tends to a finite limit, often to 0. That each graph tends to a finite limit is not a trivial result, since from covariance only the sum of all the graphs need be independent of P. There might have been cancellations between infinities of specific time-ordered graphs.

We parametrize the momentum of the i^{th} line by

$$\vec{p}_i = x_i \vec{P} + \vec{k}_i \tag{2.3}$$

where x_i is the fractional longitudinal momentum and $\vec{k}_i$ is a two-dimensional vector in the x-y plane.

Since by definition the total incident momentum is $\vec{P}$, we have

$$\sum_{inc} \vec{p}_i \equiv \left(\sum_{inc} x_i\right) \vec{P} + \sum_{inc} \vec{k}_i = \vec{P}$$

so that

$$\begin{aligned} \sum_{inc} x_i &= 1 \\ \sum_{inc} \vec{k}_i &= 0 \end{aligned} \tag{2.4}$$

Because of three-momentum conservation at each vertex, we also have for each intermediate state

$$\sum_{int} x_i = 1 \tag{2.5}$$

$$\sum_{int} \vec{k}_i = 0$$

Assuming that no photons are travelling exactly in the -z direction, we can always choose the velocity of the observing frame large enough so that all external particles have their z component of momentum positive, i.e.

$$x_i > 0 \tag{2.6}$$

for all external particles. But for internal particles, the x integrations extend over negative x as well.

In the limit $P \to \infty$, we have, from (2.2) and (2.3)

$$E_i = \sqrt{\vec{p}_i^{\,2} + m_i^2} = |x_i| P + \frac{s_i}{2P} + 0\left(\frac{1}{P^3}\right) \tag{2.7}$$

where

$$s_i = \frac{\vec{k}_i^{\,2} + m_i^2}{|x_i|} \tag{2.8}$$

The incident energy is, by (2.6) and (2.4),

$$E_{inc} = \sum_{inc} E_i = P + \sum_{inc} \frac{s_i}{2P} + 0\left(\frac{1}{P^3}\right) \tag{2.9}$$

The energy of an intermediate state is

$$E_{int} = \sum_{int} \left(|x_i| P + \frac{s_i}{2P}\right) + 0\left(\frac{1}{P^3}\right) \tag{2.10}$$

If all the x_i in the intermediate state are positive, then using (2.5) we find

$$E_{int} = P + \sum \frac{s_i}{2P} + 0\left(\frac{1}{P^3}\right) \tag{2.11}$$

If, however, some x_i are negative, we have

$$E_{int} = \left(1 - 2 \sum_{x_i < 0} x_i\right) P + 0\left(\frac{1}{P}\right) \tag{2.12}$$

Counting powers of P in a graph with n vertices, we obtain:

(a) From rule 3

$$\delta^{(3)}\left(\sum \vec{p}_i\right) = \delta^{(2)}\left(\sum \vec{k}_i\right) \delta\left(\left(\sum x_i\right) P\right)$$

$$= \frac{1}{P} \delta^{(2)}\left(\sum \vec{k}_i\right) \delta\left(\sum x_i\right)$$

and since there are (n-1) delta functions we obtain a factor $P^{-(n-1)}$.

(b) From rules 4 and 6

$$\frac{d^3 p_i}{(2\pi)^3 2E_i} = \frac{d^2 k dx}{2|x|(2\pi)^3}$$

independent of P.

(c) From rule 5 for each intermediate state with all $x_i > 0$, we obtain from (2.9) and (2.11)

$$\frac{2P}{\sum\limits_{inc} s_i - \sum\limits_{int} s_i + i\epsilon}$$

whereas if some $x_i < 0$, we obtain from (2.12),

$$\frac{1}{\left(2 \sum\limits_{x_i < 0} x_i\right) P}$$

s_i is given by (2.8). There are altogether (n-1) intermediate states, and so to obtain a non-vanishing limit as $P \to \infty$, each term from rule 5 must contribute a factor P. Thus in all cases we have a finite limit and a non-zero limit only if each intermediate state has all its $x_i > 0$. But since $\sum x_i$ is conserved at each vertex, this is only possible if each vertex has at least one line coming from the past and one line proceeding to the future. Thus, of the 6 graphs of Figure 2, only 2a and 2b have non-vanishing limits as $P \to \infty$. So the passage to infinite momentum has reduced the number of graphs to be calculated. It should be stressed that letting $P \to \infty$ is just a choice of reference frame, and no invariant quantity is getting large.

We have been rather cavalier in counting powers of P, for although P gets large, it is possible that xP is not large, and our expansion (2.7) in terms of P may not be valid. This is discussed in greater detail in Section III. Our analysis is correct for the calculation of renormalized quantities, but must be modified for calculating divergent quantities.

We can now rewrite the rules of calculation. Denoting them by primes, we obtain

1' For each Feynman graph of order n, draw all time ordered graphs in which each vertex has at least one line from the past and one to the future.

2' With each line associate an x and $\vec{k}$.

3' At each vertex except the last write a factor $(2\pi)^3 g\, \delta(\sum x_i)\delta^{(2)}(\sum \vec{k}_i)$ inserting only g at the last vertex.

5' For each intermediate state write a factor

$$\frac{2}{\sum\limits_{\text{inc}} s_i - \sum\limits_{\text{int}} s_i + i\epsilon}$$

4' and 6' Integrate

$$\frac{d^2k_i dx_i \theta(x_i)}{(2\pi)^3 2x_i}$$

7' Sum over all time ordered graphs.

The presence of spin complicates the situation. In the case of QED, the vertex becomes one of the following:[10]

$$\bar{u}(p) e\gamma^\mu u(p') \epsilon_\mu \qquad (A)$$

$$\bar{u}(p) e\gamma^\mu v(p') \epsilon_\mu \qquad (B)$$

$$-\bar{v}(p) e\gamma^\mu u(p') \epsilon_\mu \qquad (C)$$

$$-\bar{v}(p) e\gamma^\mu v(p') \epsilon_\mu \qquad (D)$$

instead of g. ($e^2 = 4\pi\alpha$). Here p and p' are the momenta of the respective on mass shell fermions (i.e., $p_0 = \sqrt{\vec{p}^2 + m^2}$), and ϵ_μ is the polarization vector of the photon.

The sum over intermediate states now also involves the sum over spin. We work in the Feynman (Gupta-Bleuler) gauge where

$$\sum_\lambda \epsilon_\mu(k, \lambda)\ \epsilon_\nu(k, \lambda) = -g_{\mu\nu}\ .$$

Our previous counting of powers of P is now upset, since the vertices can also contribute powers of P. A straightforward calculation[11] shows that as $P \to \infty$, one of the vertices (A) - (D) is of order P only if

$$\begin{aligned} &\text{(a)} \quad \mu = 0 \text{ or } 3 \text{ and } xx' > 0 \\ &\text{(b)} \quad \mu = 1 \text{ or } 2 \text{ and } xx' < 0 \end{aligned} \qquad (2.13)$$

Otherwise, it is of order 1. Moreover, in case (a), the coefficient of P is the same whether $\mu = 0$ or $\mu = 3$. (Here x and x' are the x values associated with p and p'.)

We now show that the contribution to M is of order $P^{N_1+N_3}$, where N_i is the number of external photons of polarization i.

Assume first that all $x_i > 0$, so that case (b) never arises. If a vertex is connected to an external photon, it contributes a factor P if and only if the polarization is 0 or 3. If the vertex is connected to an internal photon, because the coefficient of P is the same whether $\mu = 0$ or $\mu = 3$, and because $g_{00} = -g_{33}$ in the photon polarization sum, the terms of order P and P^2 from these two vertices cancel identically, and give an effective vertex of order 1. (The terms of order 1 do not cancel, so that one cannot say that the $\mu = 0$ piece cancels the $\mu = 3$ piece. In fact, this scalar/longitudinal piece is responsible for the Coulomb force.)

Suppose now that some $x_i < 0$. We saw that the matrix element is suppressed by $1/P^2$ for every intermediate state containing a particle with $x < 0$. But such a particle can contribute a factor P^2 to the numerator (a factor P for each of its two vertices). Thus, a fermion of negative x can contribute to M in leading order but only if (a) it extends over one time interval only, so that it contributes to only one intermediate state and (b) the fermions at each of its vertices have $x > 0$. Since a photon of negative x contributes no powers of P to the numerator, it can contribute only if every intermediate state containing it also contains a fermion of negative x. This is only possible in the simplest self energy diagram (see fig. 3) which will be discussed in Section III. These rules for incorporating fermions of negative x were first derived by Drell, Levy and Yan.[11]

Because fermions of negative x can contribute to leading order, our previous criterion of discarding graphs with fermions of negative x is no longer valid. But it can be salvaged by modifying the fermion spin sum as we now show.

The spin sum occurring in the matrix elements is

$$\sum_s u(p,s)\,\bar{u}(p,s) = (\not p + m)$$

$$\sum_s v(p,s)\,\bar{v}(p,s) = (-\not p + m).$$

Suppose there is a graph $\tilde{G}$ with a positron of momentum $\hat{p}_\mu$ with negative $\hat{x}$ between vertices V_1 and V_2 with V_2 after V_1. The energy denominator associated with the intermediate state between V_1 and V_2 is $E_{inc} - E_{int} = 2\hat{x}P$. (Note that no other particle occurring in this intermediate state can have negative x since it would extend over more than one time interval and give zero contributions. The exceptional cases are the self-energy graph of Figure 3 and the corresponding photon self-energy graph with which we will deal separately.) It is straight-forward to see that there is always an additional time-ordered graph G identical to $\tilde{G}$ except that the time order of vertices V_1 and V_2 is interchanged. The line between V_2 and V_1 now represents an electron with momentum $\vec{p} = -\vec{\hat{p}}$, $E_p = E_{\hat{p}} = \sqrt{\vec{p}^{\,2} + m^2}$. The sum of contributions from these two intermediate states

$$2P\,\frac{(\not p + m)}{s_{inc} - s_{int} + i\epsilon} + \frac{(-\hat{\not p} + m)}{2\hat{x}P} = 2P\left[\frac{(\not p + m)}{s_{inc} - s_{int} + i\epsilon} + \frac{-2E_p\gamma^0}{4\hat{x}P^2} + \frac{\not p + m}{4\hat{x}P^2}\right] \tag{2.14}$$

The third term of (2.14) is negligible compared to the first. Also we have

$$E_p = |\hat{x}|P = -\hat{x}P \qquad \text{since } \hat{x} < 0 \tag{2.15}$$

and so (2.14) becomes

$$2P \left[\frac{\tilde{\not{p}} + m}{s_{inc} - s_{int} + i\epsilon} + 0 \left(\frac{1}{P^2} \right) \right] \tag{2.16}$$

where

$$\vec{\tilde{p}} = \vec{p}$$

$$\tilde{p}^0 = p^0 + \frac{s_{inc} - s_{int}}{2P} . \tag{2.17}$$

By changing the propagator of an electron with positive x from $(\not{p} + m)$ to $(\tilde{\not{p}} + m)$ whenever the electron line extends over a single time interval, we automatically take into account the contribution of all positrons with $x < 0$. Similarly, we modify the propagator of positrons with positive x, which extends over one time interval, from $(-\not{p} + m)$ to $(-\tilde{\not{p}} + m)$. We do not change the propagators of fermion lines extending over more than one time interval. With the replacement (2.17) only time-orders in which every intermediate state has positive-moving particles needs to be explicitly considered.

This replacement of p_μ by $\tilde{p}_\mu$ is very reminiscent of the Feynman approach. One takes the fermion off the mass shell ($\tilde{p}^2 \neq m^2$), but reduces the number of diagrams. Moreover, $\tilde{p}_\mu$ is the four-vector which enforces four-momentum conservation between the given intermediate state and the <u>external</u> state:

$$(E_{int} - p_0) + \tilde{p}_0 = E_{inc} .$$

However, since not all fermion lines extend over a single time interval we do not have complete four-momentum conservation at every vertex.

From (2.13b) we see that it is not necessary to modify the propagator of a fermion extending over a single time interval if either of its vertices is connected to an external photon of polarization 0 or 3, although modifying it will not change the answer. This follows because the associated fermion of negative x cannot contribute the necessary P^2 to the numerator.

Our final rules for QED at infinite momentum are thus obtained by modifying the infinite momentum rules for the ϕ^3 theory as follows:

2'' With each internal line associate an x and k. For $\binom{\text{electrons}}{\text{positrons}}$ extending over more than one time interval insert a factor $(\pm\not{p} + m)$ where p is the four momentum associated with the line. For fermions extending over <u>one</u> time interval insert the factor $(\pm\widetilde{\not{p}} + m)$ where $\widetilde{p}$ is related to p by (2.17). For each internal photon line insert the factor $-g_{\mu\nu}$. A trace is implied for closed fermion loops.

3'' Replace g by $e\gamma^{\mu}$ in 3'.

Finally, we note that if we assign momenta $p_1, \cdots p_N$ for the fermion momenta of a given graph, then the Dirac algebra for each time-ordering is identical to that of the Feynman graph calculation, although the identification of p_i in terms of the external and loop momenta depends on the particular time-order.

III. RENORMALIZATION

In this section we indicate how to implement the renormalization procedure in TOPTh_{∞}. This procedure is simple and straightforward to apply in practice, and closely parallels the explicitly covariant Feynman-Dyson approach. Reducible amplitudes with self-energy and vertex insertions are renormalized using subtraction terms corresponding to δ_m, Z_2 and Z_1 counter terms, which usually can be constructed to cancel pointwise the ultraviolet d^2k phase-space integrations. In this section we develop the renormalization procedure for QED in TOPTh_{∞} and concentrate on the features which are distinct to the infinite momentum method. In the next section we discuss the application of these rules to the calculation of the electron anomalous moment in fourth order. Here we present a heuristic proof of the renormalizability of QED and discussion of the uniformity of the $P \to \infty$ limit.

In performing these renormalizations, we are subtracting infinite quantities, which is always a delicate procedure. The correct way to do so is to first regulate the integrals, rendering them finite, then subtract, and then let the regulators disappear. In the infinite momentum frame, since covariance is not manifest, one must be especially careful to regulate in an invariant manner. This can be achieved by using the Pauli-Villars regularization scheme.

A. Self Energy Insertion in Compton Scattering

As a first simple example consider the self-energy insertion to Compton scattering shown in Figure 4. In the usual Feynman approach the renormalized amplitude is constructed by subtracting formally divergent δ_m and Z_2 counter terms in second order. The problem is to choose an integral representation for these constants so that the total integrand of the renormalized amplitude is finite and point-wise covergent. In general, the integrands are defined assuming covariant Feynman or Pauli-Villars regularization.

The frame is chosen so that the fermion line p_a in figure 4 has momentum $\vec{p}_a = \vec{P}$. For the moment, consider the case of scalar particles. Only one time-order survives as $P \to \infty$. The unrenormalized amplitude is

$$M_u = \frac{g^4}{2(2\pi)^3} \int d^2k \int_0^1 \frac{dx}{x(1-x)} \left[\frac{1}{s_0-s_1} \; \frac{1}{s_0-s_2} \; \frac{1}{s_0-s_3} \right] \qquad (3.1)$$

where (using a photon mass λ)

$$s_0 = (p_1 + q_1)^2 + i\epsilon$$

$$s_1 = m^2 = s_3 \tag{3.2}$$

$$s_2 = \frac{\vec{k}^2 + \lambda^2}{x} + \frac{\vec{k}^2 + m^2}{1 - x}$$

The δ_m and $Z_2 = 1+B_{(2)}$ counter terms subtractions may be computed by what we call the method of alternate denominators. Note that δ_m can be written as

$$\delta_m = \frac{g^2}{2(2\pi)^3} \int d^2k \int_0^1 \frac{dx}{x(1-x)} \frac{1}{s_1 - s_2 + i\epsilon} \tag{3.3}$$

since particle a is on the mass-shell. [Note this expression must be defined here by covariant-regularization, e.g., by subtraction of a heavy photon of mass Λ^2.] Thus mass-renormalization only requires the subtraction of the integrand with the alternate denominator

$$\frac{1}{s_0 - s_1} \frac{1}{s_1 - s_2} \frac{1}{s_0 - s_3} \tag{3.4}$$

in M_u. Similarly, if we perform wavefunction renormalization we obtain the renormalized amplitude

$$M_{ren} = \frac{g^4}{2(2\pi)^3} \int_0^1 dx \int \frac{d^2k}{x(1-x)} \left[\frac{1}{(s_0-s_1)(s_0-s_2)(s_0-s_3)} - \frac{1}{(s_0-s_1)(s_1-s_2)(s_0-s_3)} \right.$$
$$\left. + \frac{1}{(s_0-s_1)(s_1-s_2)^2} \right] \tag{3.5}$$

The last term is exactly $-B^{(2)}$ times the Born term. The total integrand is now rendered finite in the ultraviolet ($\vec{k}^2 \to \infty$). By combining the terms, we see that the single particle poles disappear, so that the location and residue of Compton scattering is still given by the Born term.

The essential point of the "alternate denominator" method is that the external energy used for the denominator of the subtraction term for a reducible insertion is not the external (initial) energy s_0 but rather the energy (s_1) external to that reducible subgraph. The analogue to off-mass shell behavior in the Feynman approach is precisely the difference between the use of s_0 and s_1 in the energy denominators. In general, in self energy insertions onto a line with momentum $\vec{p}_a$ one should use the "scaled" variables $\vec{\ell}_1 = x\vec{p}_a + \vec{k}$, and $\vec{\ell}_2 = (1-x)\vec{p}_a - \vec{k}$ for the internal integration. This will ensure point-wise convergence of the d^2k integration, after subtraction of the necessary counter terms.

Combining terms in M_{ren} we obtain the covariant spectral form

$$M_{ren} = \frac{g^4}{2(2\pi)^3} \int d^2k \int_0^1 \frac{dx}{x(1-x)} \frac{1}{(s_1-s_2)^2} \frac{1}{s_0-s_2} \tag{3.6}$$

$$= \int_{(m+\lambda)^2}^{\infty} d\mu^2 \rho(\mu^2) \frac{g^2}{(p+q)^2 - \mu^2 + i\epsilon} \tag{3.7}$$

where $\mu^2 = s_2$ and

$$\rho(\mu^2) = \frac{g^2}{16\pi^2} \frac{1}{(m^2-\mu^2)^2} \int_0^1 dx \quad \theta\,[x(1-x)\mu^2-(1-x)\lambda^2-xm^2] \tag{3.8}$$

$$= \frac{g^2}{16\pi^2} \frac{1}{(m^2-\mu^2)^2} \frac{\sqrt{(\mu^2+\lambda^2-m^2)^2-4\mu^2\lambda^2}}{\mu^2} \tag{3.9}$$

Thus the renormalization is identical to that obtained by using the spectral integral of the renormalized Feynman propagator, since $\pi\rho(\mu^2) = \mathrm{Im}\, D_F^{ren}(\mu^2)$.

B. Vacuum Polarization

Consider the vacuum polarization insertion in electron-electron scattering [Figure 5a]. If we choose a frame in which $\vec{q} = \vec{p}_1 - \vec{p}_2$ has a positive component along $\vec{P}$, then only the time order in which the (q, p_1, p_2) vertex occurs first and the (q, p_3, p_4) vertex occurs last contributes for $P \to \infty$. The energy denominator for any intermediate state inside the vacuum polarization insertion is

$$\frac{1}{E_1+E_3-[E_2+E_3+\sum\limits_{\substack{\text{vac.}\\\text{pol.}}} E_i]} = \frac{1}{E_1-E_2-\sum\limits_{\substack{\text{vac.}\\\text{pol.}}} E_i}, \tag{3.10}$$

so that the initial energy for the vacuum polarization insertion is $\tilde{q}_0 \equiv p_1^0 - p_2^0$. Thus if we define $q_F^2 = (p_1-p_2)^2$, then the amplitude has the factorized Feynman form

$$M = g^2 \frac{1}{(q_F^2-\lambda^2+i\epsilon)^2} \pi_u(q_F^2) \tag{3.11}$$

where $\pi_u(q_f^2)$ is computed from diagram 5(b), for a photon mass $q_F^2 < 0$. The Feynman propagator $q_F^2 - \lambda^2 + i\epsilon$ is obtained from the product of the photon phase space $(2q_0)^{-1}$ and the energy denominator $(p_{10}-p_{20}-q_0+i\epsilon)^{-1}$ at infinite momentum.

Renormalization may now be carried out by the alternate denominator method as in section A. The renormalized amplitude is then a spectral integral of the Born amplitude over photon mass which we shall calculate below. We can easily extend the analysis to self-insertion in higher order graphs. For example, consider the time-ordered contributions to electron-electron scattering shown in Figure 6. After the integrand for the counter terms for the vacuum polarization insertion are computed using the alternate energy denominator method, one finds that the three time orders combine simply and the renormalized amplitude can again be written as the spectral integral in photon mass over the "Born" amplitude of Figure 7.

As a further example, we calculate the lowest order vacuum polarization correction to lepton-lepton scattering in QED. The sum of the contributions from Figure 8 is

$$\ell_1^\alpha \ell_2^\beta \left[\frac{-g_{\alpha\beta}}{q_F^2 + i\epsilon} + \frac{(-g_{\alpha\mu})(-g_{\nu\beta})}{(q_F^2 + i\epsilon)^2} \pi^{\mu\nu} \right] \tag{3.12}$$

where by Lorentz invariance $\pi^{\mu\nu}$ is a function of $q_F^\mu = p_1^\mu - p_2^\mu$ and by gauge-invariance, $\pi^{\mu\nu}$ has the form

$$\pi^{\mu\nu} = (-g^{\mu\nu} q_F^2 + q_F^\mu q_F^\nu)\, \pi(q^2) \tag{3.13}$$

and ℓ_1 and ℓ_2 are the lepton current factors. At infinite momentum we can extract $\pi(q^2)$ from $\pi_{\mu\nu}$ simply by considering

$$\pi_{03} = q_0 q_3 \pi(q^2). \tag{3.14}$$

Moreover, choosing

$$q = \left(P + \frac{q^2}{2P} \;, \; \vec{0}, \; P \right) \tag{3.15}$$

we see that

$$\pi(q^2) = \lim_{P\to\infty} \frac{\pi_{03}(q^2)}{P^2} . \tag{3.16}$$

Only the piece of π_{03} proportional to P^2 survives, and graph 8(c) is eliminated. Restricting our attention to graph 8(b), we have

$$\pi_{03} = \frac{e^2}{2(2\pi)^3} \int_0^1 dx \int \frac{d^2k}{x(1-x)} \; \frac{\mathrm{Tr}[(m+\not{p}_1)\gamma^0(m-\not{p}_2)\gamma^3]}{q_F^2 - \frac{\vec{k}^2+m^2}{x} \; \frac{\vec{k}^2+m^2}{1-x} + i\epsilon} \tag{3.17}$$

where p_1 and p_2 are on-shell with space components $(\vec{k}, xP)$ and $(-\vec{k}, (1-x)P)$ respectively. The term proportional to P^2 gives the unrenormalized amplitude

$$\pi(q_F^2) = \lim_{P\to\infty} \frac{\pi_{03}}{P^2} = \frac{4e^2}{(2\pi)^3} \int_0^1 dx \int d^2k \, \frac{x(1-x)}{\vec{k}^2+m^2-q_F^2 x(1-x)-i\epsilon} \tag{3.18}$$

We obtain the renormalized amplitude by subtraction at $q^2 = 0$ (corresponding to wavefunction renormalization of the photon) or by alternate denominators. Thus

$$\pi_{ren}(q_F^2) = \frac{2\alpha}{\pi} \int_0^1 dx \, x(1-x) \log \left[1 - \frac{q_F^2 x(1-x)}{m^2-i\epsilon}\right] \tag{3.19}$$

and the total lepton-lepton scattering interaction for Figure 8 is

$$\ell_1^\mu \ell_2^\nu \frac{(-g_{\mu\nu})}{q_F^2-\lambda^2+i\epsilon} [1 + \pi_{ren}(q^2)] \tag{3.20}$$

in agreement with the standard results.

C. Vertex Factorization

Before discussing vertex renormalization, we first give a general proof of vertex factorization in TOPTh_∞. Consider the scattering diagram of Figure 9 in which the vertex part contains a total of N+1 internal interactions. For simplicity we continue to treat all the particles as spinless.

We choose q to have positive momentum in the $\vec{P}$ direction. If q attaches to an internal line after m internal interactions have occurred ($0 \le m \le N$), then there are m+1 contributing time-orders depending on the time of the (p_1, p_2, q) interaction. Since q is on the mass shell, $q_0 = \sqrt{\vec{q}^2+\lambda^2}$. We also define

$\tilde{q}_0 = p_1^0 - p_2^0 = p_4^0 - p_3^0$. Summing over the m+1 contributions yields the integrand factor

$$F_m = \frac{1}{\tilde{q}_0 - q_0} \frac{1}{\tilde{q}_0 + \Delta e_1 - q_0} \frac{1}{\tilde{q}_0 + \Delta e_2 - q_0} \cdots \frac{1}{\tilde{q}_0 + \Delta e_m - q_0}$$

$$+ \frac{1}{\Delta e_1} \frac{1}{\tilde{q}_0 + \Delta e_1 - q_0} \frac{1}{\tilde{q}_0 + \Delta e_2 - q_0} \cdots \frac{1}{\tilde{q}_0 + \Delta e_m - q_0}$$

$$+ \frac{1}{\Delta e_1} \frac{1}{\Delta e_2} \frac{1}{\tilde{q}_0 + \Delta e_2 - q_0} \cdots \frac{1}{\tilde{q}_0 + \Delta e_m - q_0}$$

$$+ \cdots + \frac{1}{\Delta e_1} \frac{1}{\Delta e_2} \cdots \frac{1}{\Delta e_m} \frac{1}{\tilde{q}_0 + \Delta e_m - q_0}$$

$$= \frac{1}{\tilde{q}_0 - q_0} \prod_1^m \frac{1}{\Delta e_j} \tag{3.21}$$

where Δe_1 is the i^{th} energy denominator specific to the vertex. The remaining energy denominators give the common factor

$$\prod_{j=m+1}^{N} \frac{1}{\Delta e_j + \tilde{q}_0} \tag{3.22}$$

The phase space factor for the photon $2q_0$ combines with the factor $(\tilde{q}_0 - q_0)$ to give the Feynman propagator,

$$2q_0(\tilde{q}_0 - q_0) = (p_1 - p_2)^2 - \lambda^2 + i\epsilon \equiv q_F^2 - \lambda^2 + i\epsilon \tag{3.23}$$

Thus, as expected, for each m the scattering amplitude takes the Feynman factorized form

$$M = \frac{g}{\tilde{q}^2 - \lambda^2 + i\epsilon} F(\tilde{q}^2) \, . \tag{3.24}$$

where $F(\tilde{q}^2)$ is the vertex graph computed with the photon mass given formally by $\tilde{q}^2 = (p_1 - p_2)^2 < 0$. Note that pair creation graphs also have the form (3.24).

Thus, the concept of virtual-mass particles and the factorization of vertex form factors appears naturally in TOPTh_∞ when the appropriate time-orders are summed over. This also permits by covariance the use of the special frame choice[4]

$$q^\mu = \left(\frac{q\cdot P}{P}, \vec{q}, 0\right), \quad q^2 = -\vec{q}^{\,2} < 0 \tag{3.25}$$
$$P = \left(P + \frac{m^2}{2P}, \vec{0}, P\right)$$

which is very convenient for calculations of the virtual Compton amplitude ($2q\cdot P = m\nu$) and form factor ($2q\cdot P = -q^2$). In this frame, $\vec{q}$ brings in zero longitudinal momentum, eliminates pair-creation graphs, and thus further reduces the number of contributing time-orders.

D. <u>Ward Identity</u>

The use of frame (3.25) allows an immediately proof of the Ward identity $Z_1 = Z_2$ for the cancellation of vertex and wave function renormalization in QED. We define the form factors as

$$\langle p+q\,|J^\mu(0)|\,p\rangle = \bar{u}(p+q)\left[F_1(q^2)\gamma^\mu + i\,\frac{\sigma^{\mu\nu}q_\nu}{2m}\,F_2(q^2)\right]u(p)\,. \tag{3.26}$$

At t=0 we may identify $J_\mu(0) = j_\mu(0) = :\bar{\psi}\gamma_\mu\psi:$, the free current, in the interaction picture, and compute F_i by TOPTh. Let us concentrate here on computing the contribution to Z_1 or $F_1(0)$ from any given proper vertex diagram in TOPTh. Note that for q=0

$$F_1(0) = \lim_{P\to\infty} \langle p|\,j_\mu(0)\,|p\rangle\,\frac{m}{P} \qquad (\mu = 0, 3) \tag{3.27}$$

Thus the contribution to Z_1 from any proper vertex graph is obtained by simply inserting $(m/P)\gamma_0$ or equivalently x at the interaction vertex, where x is the fractional longitudinal momentum of the interacting charged line. This factor of x cancels against one of the two phase-space forms of x^{-1} required for that line. The resulting expression is then identical to that required for computing the contribution of the corresponding proper diagram to the wave function renormalization constant Z_2 for the state $|p\rangle$. The result $Z_1 = Z_2$ then holds to our order in perturbation theory. The same simple proof holds in the case where $|p\rangle$ is a bound state.

E. Vertex Renormalization

As a final simple example of the alternate denominator renormalization procedure in QED, consider the renormalization of the vertex insertion in the ladder graph contribution to the electron anomalous magnetic moment $F_2(0)$. If we choose the (symmetrized) frame

$$q^\mu = (0, \vec{q}, 0), \quad (p \pm \tfrac{q}{2}) = \left(P + \frac{m^2 + \frac{\vec{q}^{\,2}}{2}}{2P}, \pm \frac{\vec{q}}{2}, P\right), \quad q^2 = -\vec{q}^{\,2}$$

then only the single time-order shown in Figure 10 needs to be explicitly considered at $P \to \infty$. [Recall that backward-moving fermion contributions are included automatically by modifying the fermion spin sum (2.17).] As in the Feynman calculation the integration of the reducible subgraph is logarithmically divergent in the ultraviolet. The subtraction of the contribution $\frac{\alpha}{2\pi} L^{(2)}$ is required, where $\gamma_\mu L^{(2)}$ is the value of the proper vertex at $q = 0$ in second order. The unrenormalized amplitude is

$$M_u = \frac{e^4}{4(2\pi)^6} \int_0^1 dx_1 dx_2 \int \frac{d^2k_1 d^2k_2}{x_1(1-x_1)^3 x_2(1-x_2)^2}$$

$$\frac{\bar{u}(p+\frac{q}{2})\gamma_\alpha(\tilde{\not{p}}_4+m)\gamma_\beta(\tilde{\not{p}}_3+m)\gamma_\mu(\tilde{\not{p}}_2+m)\gamma^\beta(\tilde{\not{p}}_1+m)\gamma^\alpha u(p-\frac{q}{2})}{(s_0-s_1)(s_0-s_2)(s_0-s_3)(s_0-s_4)} \tag{3.28}$$

where we choose the parameterization

$$\vec{\ell}_1 = \vec{k}_1 + x_1\vec{P}, \quad \vec{\ell}_2 = \vec{k}_2 + x_2\,(-\vec{k}_1 + (1-x_1)\vec{P})$$

for the three-momentum of the two photons. The fermion momenta then are determined by three-momentum conservation. With this choice of scaled variables the range of both x_1 and x_2 is 0 to 1 and $\vec{k}_1 \cdot \vec{k}_2$ cross terms do not appear. Notice that the denominator product in (3.28) is an even function of $\vec{q}$ because of the choice of the symmetrized frame. In the calculation of $F_2(0)$, the magnetic moment contribution is identified[12] from a term linear in $\vec{q}$ and the $\vec{q}$ dependence of the denominators may be dropped.

The subtraction term is constructed using the alternate denominators $(s_1-s_2)(s_1-s_3)$ instead of $(s_0-s_2)(s_0-s_3)$ and the appropriate numerator coefficient of γ_μ at $q \to 0$:

$$M_{sub} = \frac{e^4}{4(2\pi)^6} \int_0^1 dx_1 dx_2 \int \frac{d^2k_1 d^2k_2}{x_1(1-x_1)^3 x_2(1-x_2)^2}$$

$$\frac{\bar{u}(p+\frac{q}{2})\gamma_\alpha(\tilde{p}_4+m)\gamma_\mu(\tilde{p}_1+m)\gamma^\alpha u(p-\frac{q}{2})}{(s_0-s_1)(s_0-s_4)} \left[\frac{(8m^2-4p_1\cdot p_2)(1-x_2)}{(s_1-s_2)(s_1-s_3)}\right]_{q\to 0} \tag{3.29}$$

The last factor is the integrand for $L^{(2)}$ in second order. The difference

$$M_{ren} = M_u - M_{sub}$$

converges point wise in the d^2k integrations, and contributes a finite amount to $F_2(0)$. The infrared behavior [at $x_1 \sim 0$ in M_u and $x_2 \sim 0$ in M_{sub}] may be regulated by using a finite photon mass λ as in the Feynman calculation. In the case of the ladder graph contribution to $F_2(0)$, these two infrared terms in fact cancel. The cancellation may be arranged to happen pointwise in the integrand by symmetrizing the $(\vec{k}_1, x_1)$ and $(\vec{k}_2, x_2)$ integration of M_{ren}.

F. The Renormalization Constants

The calculation of δm_e in second order is an excellent illustration of the subtleties of the limit $P \to \infty$. As we have already indicated, our rule for incorporating fermions of negative x is not valid in this case, so we revert to the older rules in which particles of negative x are treated explicitly. Then there are 2 graphs, as indicated in figure 11a and 11b. As is well known these graphs are divergent and have to be regulated. A naive argument would say that, upon photon regularization, graph (11b) vanishes, for since at least one of the particles in the intermediate state has $x < 0$, the energy denominator is just $\frac{1}{1 - \sum_{int} |x_i|}$ independent of the photon mass. Consequently, subtracting a similar integrand with a large photon mass will give identically zero.

Unfortunately, the argument is wrong, because the limit $P \to \infty$ cannot be taken under the integral sign. One must integrate first and only then let $P \to \infty$.

To see this, let us define the $P \to \infty$ rules more carefully. Ignoring the numerator structure for the moment, the denominators are, before we take $P \to \infty$,

$$\frac{1}{e_k} \; \frac{1}{E_{-p-k}} \; \frac{1}{E - e_k - E_{-p-k}} \tag{3.30}$$

where

$$\begin{aligned} e_k &= \sqrt{(xP)^2 + \vec{k}^2 + \lambda^2} \\ E_{-p-k} &= \sqrt{(1-x)^2 P^2 + \vec{k}^2 + m^2} \\ E &= \sqrt{P^2 + m^2} \end{aligned} \tag{3.31}$$

and λ is a small photon mass.

For large P we wrote

$$e_k = |x| P + \frac{\vec{k}^2 + \lambda^2}{2|x|P} \tag{3.32}$$

and disregarded the second term in (3.32) in the first term of (3.30). This is legitimate provided that the function multiplying $\frac{1}{e_k}$ vanishes at x = 0, so that the integral over x is well defined. In other words as a distribution on functions vanishing at x = 0 we have

$$\frac{1}{e_k} \rightarrow \frac{1}{|x|P} \tag{3.33}$$

for large P. But if the functions vanish at x = 0, we could also write

$$\frac{1}{e_k} \rightarrow \frac{1}{|x|P} + \frac{C\delta(x)}{P} \tag{3.34}$$

To fix the coefficient C, consider what happens if the function does not vanish at x = 0. Then the integral is not well defined and must be regulated, by subtracting the contribution of a heavy photon. So we must study

$$\lim_{P\rightarrow\infty} \quad \frac{P}{\sqrt{(xP)^2 + \vec{k}^2 + \lambda^2}} - \frac{P}{\sqrt{(xP)^2 + \vec{k}^2 + \Lambda^2}} \tag{3.35}$$

where Λ is the mass of the regulator photon. For $x \neq 0$ this limit vanishes. But it is readily checked that as a distribution in x, (3.35) tends to

$$-\ln\left(\frac{\vec{k}^2 + \lambda^2}{\vec{k}^2 + \Lambda^2}\right)\delta(x) \tag{3.36}$$

This is consistent with (3.34) if

$$C = -\ln(\vec{k}^2 + \lambda^2). \tag{3.37}$$

One might argue that

$$\frac{P}{e_k} = \frac{1}{\sqrt{x^2 + (\vec{k}^2 + \lambda^2)/P^2}} \tag{3.38}$$

is not a function of $(k^2 + \lambda^2)$, but of $\frac{\vec{k}^2 + \lambda^2}{P^2}$, so that C should be $-\ln\left(\frac{\vec{k}^2 + \lambda^2}{P^2}\right)$.

But on regularization the $\ln P^2$ terms cancel. Using then as the energy term

$$\frac{P}{e_k} = \frac{1}{|x|} - \ln(\vec{k}^2 + \lambda^2)\delta(x) \tag{3.39}$$

one shows that 11b does give a contribution upon regularization.

By our rules after regularization the contribution of diagram 11a to δm is

$$\delta m_a = \frac{e^2}{16\pi^3 m} \int d^2k \int_0^1 \frac{dx}{(1-x)} \left\{ \frac{m^2(2-2x-x^2)-\vec{k}^2}{\lambda^2(1-x)+\vec{k}^2+m^2x^2} - (\lambda \rightarrow \Lambda) \right\} \tag{3.40}$$

where the photon mass is taken to be λ, and its longitudinal and transverse momenta are xP and $\vec{k}$.[13]

Our new rule for δm_b gives

$$\delta m_b = -\frac{e^2}{16\pi^3 m} \int d^2k \left\{ \ln(\vec{k}^2 + \lambda^2) - \ln(\vec{k}^2 + \Lambda^2) \right\} . \tag{3.41}$$

Combining these two terms yields the Feynman result, which can be written as

$$\delta m_F = \frac{e^2}{16\pi^3 m} \int d^2k \int_0^1 dx \left\{ \frac{2m^2(1+x)}{\vec{k}^2+m^2x^2+(1-x)\lambda^2} - (\lambda \leftrightarrow \Lambda) \right\}. \tag{3.42}$$

This can be obtained by substituting the identity

$$\ln(\vec{k}^2 + \lambda^2) - \ln(\vec{k}^2 + \Lambda^2) = \ln\left(\frac{\vec{k}^2+\lambda^2}{\vec{k}^2+m^2}\right) - \ln\left(\frac{\vec{k}^2+\Lambda^2}{\vec{k}^2+m^2}\right)$$

$$= \int_0^1 \left\{ \frac{\lambda^2 - 2m^2x}{\vec{k}^2+m^2x^2+(1-x)\lambda^2} - (\lambda \leftrightarrow \Lambda) \right\} dx \tag{3.43}$$

into δm_b. Another derivation of this result is given in the Appendix.

It is clear that for amplitudes which are already finite, the $\delta(x)$ cannot contribute and our previous rules are correct. Thus, for example, in calculating the contribution of figure 12 (and the corresponding δ_m counterterms of figure 13) to the magnetic moment of the electron, the contributions of Figures 12b and 13b cancel identically upon regularizaion. For renormalized amplitudes only figure 11a contributes to the self energy insertion.

It should be noted, that technically, if the Pauli principle were taken into account, graph 11b would not contribute to δ_m since the intermediate state has two electrons of the same momentum and spin. In fact, the actual contribution of interest is the vacuum disconnected graph 11c,where the entire Figure 11c d^4p integration would give no physical contribution, except for the fact that the $p_1 = p$ contribution is missing. However, 11c gives the same contribution as 11b calculated as if the Pauli principal is ignored. This is clear since we can imagine taking $p' = p+\delta$ in 11b by considering an off-shell process. The sum of 11b and 11c is continuous as $\delta \rightarrow 0$. Accordingly we can follow the usual Feynman convention of ignoring the Pauli principal and the contribution of vacuum disconnected amplitudes. In the case of the unrenormalized amplitude for the vertex graph of figure 14, a $\delta(1-x)$ contribution will occur. [This disagrees with the argument given in ref. 5, that all distribution-type terms can be associated with vacuum disconnected graphs.] However, upon regularization in the photon mass this contribution cancels, and it never appears in the renormalized amplitude. We note also that if regularization in the lepton mass is used in the δ_m calculation, then the $\delta(x)$ contributions may be formally ignored.

G. Renormalizability

It is possible to give a heuristic proof of renormalizability of various theories directly from TOPTh in the infinite moment frame. The ultraviolet divergences of the phase-space integrations are assumed to be covariantly regulated by gauge-invariant Pauli-Villars negative metric internal leptons or photons (or by Feynman spectral conditions) where required. The infrared behavior at $x_{photon} \sim 0$ may be regulated by using a photon mass λ^2.[14] We use the Weinberg power-counting theorem.[15] After removal of divergent subgraphs, the phase-space integrals of the skeleton graph will converge in the ultraviolet if the total degree of divergence d is negative.

We begin with the ϕ^3 theory. Recall that the degree of divergence in the Feynman theory is, for a graph with V vertices and N internal lines

$$\underbrace{4N}_{\text{from } d^4k} - \underbrace{2N}_{\substack{\text{from the}\\ \text{propagators}}} - \underbrace{4(V-1)}_{\substack{\text{from momentum}\\ \text{conservation}}}$$

while in our rules it is

$$\underbrace{2N}_{\text{from } d^2k} - \underbrace{2(V-1)}_{\substack{\text{from energy}\\ \text{denominators}}} - \underbrace{2(V-1)}_{\substack{\text{from momentum}\\ \text{conservation}}}$$

which agrees with the Feynman result. Thus, just as in the Feynman case, one proves the renormalizability of the theory.

For any Feynman diagram in spin 1/2 QED, one finds from the usual Feynman rules

$$d_{1/2} = \underbrace{4(B_i+F_i)}_{(\text{from } d^4k)} - \underbrace{(F_i+2B_i)}_{\substack{(\text{from}\\ \text{propagators})}} - \underbrace{4(V-1)}_{\substack{(\text{from momentum}\\ \text{conservation})}}$$

$$= 4 - \frac{3}{2} F_e - B_e$$

where B_i, B_e, F_i, F_e denote the number of internal and external bosons and fermions.[16] For spin zero electrodynamics, we have

$$\begin{array}{rccccccc} d_0 & = & 4(B_i + F_i) & + \; V & - & (2F_i + 2B_i) & - & 4(V-1) \\ & & \text{(from } d^4k) & \text{(numerator terms)} & & \text{(from propagators)} & & \text{(from momentum conservation)} \\ & = & 4 - F_e - B_e \, . \end{array}$$

The only difficulty in deriving analogous rules for spin 1/2 QED in TOPTh_∞ is in deciding the number of powers of k contributed by the spin sums $\not{p}_i + m_i$ or $\tilde{\not{p}}_i + m_i$. For each internal fermion line, these spin sums contribute one power of $|\vec{k}|$ from $\vec{\gamma} \cdot \vec{k}$. If any two of these internal vectors dot together, this rule is correct since the result is of order $\vec{k}^2$. If however, such a p_i dots with an external line, the contribution is of order $\vec{k}^2$, not $|\vec{k}|$. We now show that this can contribute at most an extra factor $|\vec{k}|^{Fe/2}$.

This situation arises in computing

$$\bar{u}(p'')\mathcal{M}\, u(p')$$

where p', p'' are external fermion momenta and $\mathcal{M}$ is formed from scalars and $\not{p}_i$. It can be verified that the combination

$$p_1 \cdot p'' \quad p_2 \cdot p'$$

cannot occur in such a term, except in the combination

$$(p_1 \cdot p''\, p_2 \cdot p' - p_2 \cdot p''\, p_1 \cdot p')$$

which is at most of order $\vec{k}^3$, and not of order $\vec{k}^4$. This is a reflection of the fact that two spin 1/2 spinors (of momentum p', p'') cannot couple to a spin 2 object, as is required to produce the symmetric tensor $p'_\mu p''_\nu$. As a result, for each two external fermions, the degree of $\vec{k}$ in the matrix element can only be increased by 1. Thus the powers of $\vec{k}$ contributed by the spin sums is at most

$$F_i + \frac{F_e}{2} .$$

Then we obtain, for each time order diagram in spin 1/2 QED, the degree of divergence

$$d_{1/2} = \underset{(\text{from } d^2k_i)}{2(B_i + F_i)} + \underset{(\text{numerator terms})}{(F_i+F_e/2)} - \underset{(\text{energy denominators})}{2(V-1)} - \underset{(\text{momentum conservation})}{2(V-1)}$$

$$= 4 - F_e - B_e .$$

Similarly, for spin-0, TOPTh QED at infinite momentum

$$d_0 = \underset{(\text{from } d^2k_i)}{2(B_i + F_i)} + \underset{(\text{numerator terms})}{V} - \underset{(\text{energy denominators})}{2(V-1)} - \underset{(\text{momentum conservation})}{2(V-1)}$$

$$= 4 - F_e - B_e .$$

Since d depends on the number of external lines, there are a finite number of divergent subgraphs and the usual renormalization program may be carried out. Note that the result for $d_{1/2}$ is an over-estimate since, as the Feynman result shows, the extra $F_e/2$ in $d_{1/2}$ cancels when the various time-orderings are combined.

This cancellation (between pair states and non-pair states) can be traced to Fermi statistics.

H. Convergence as $P \to \infty$

We restrict our attention to ϕ^3 theories. We have already shown in the previous section that the degree of divergence in $\vec{k}^2$ is as in the Feynman theories, and it is easily seen that there is no divergence in x, since the factor $\frac{1}{x}$ associated with each line is compensated by the factor $\frac{\vec{k}^2 + m^2}{x}$ appearing in the energy denominator of the intermediate states in which this line occurs.

We discarded contributions of particles with negative x because the energy denominators formally suppressed the graph by $1/P^2$. But the effective energy denominator

$$\frac{1}{P^2} \qquad \frac{1}{1 - \sum\limits_{\text{int}} |x_i|}$$

does not contain the factor x/k^2 which we counted on in our previous analysis, so that one could get divergence at $x = 0$ or $k^2 = \infty$. To study these recall that the energy denominator is really

$$\frac{1}{P^2} \qquad \frac{1}{1 - \sum |x_i| + \sum\limits_{\text{inc}} \frac{\vec{k}_i^2 + m_i^2}{2x_i P^2} - \sum\limits_{\text{int}} \frac{\vec{k}_i^2 + m_i^2}{2|x_i|P^2}} \tag{3.44}$$

If only x_1 is negative, then as it goes to zero the term is

$$\frac{1}{P^2} \qquad \frac{1}{2x_1 + 0\left(\frac{1}{x_1 P^2}\right)} \tag{3.45}$$

The $0\left(\frac{1}{x_1 P^2}\right)$ term cuts off the integral at $x_1 = 0\left(\frac{1}{P}\right)$. The contribution to the graph from small x_1 is then

$$\frac{1}{P^2} \int\limits_{|x_1| > \frac{1}{P}} \frac{dx_1}{|x_1|} \frac{1}{2x_1} \approx 0\left(\frac{1}{P}\right) \tag{3.46}$$

and so is still negligible. By a similar argument the $\vec{k}^2$ integral is cut off at P^2 (actually $\vec{k}^2 = xP^2$). If the rest of the graph contributes a factor $\frac{1}{\vec{k}^2}$ then the entire contribution is

$$\frac{1}{P^2} \int_{\vec{k}^2 < P^2} \frac{d^2k}{\vec{k}^2} = \frac{-\ell n P^2}{P^2} \tag{3.47}$$

which is still negligible. If however, there is no other factor $1/\vec{k}^2$ the graph contributes

$$\frac{1}{P^2} \int_{\vec{k}^2 < P^2} d^2k = 0(1) \tag{3.48}$$

and is <u>not</u> negligible. This only happens if the vector k does not occur in any other intermediate state, for otherwise the energy denominator of that state would have a factor $1/\vec{k}^2$. But this can only happen in the lowest order self energy graphs or in any graph in which these are imbedded. These are self energy terms which must be regulated anyway, by subtracting the contribution of a heavy mass M. One verifies that after regularization the contribution of negative x can be discarded.

In summary, our $P = -\infty$ rules are valid for renormalized quantities but not for unrenormalized ones.

IV. CALCULATIONS

As an example of these techniques, we have calculated the 4th order contribution to the magnetic moment of the electron in QED. We chose this particular calculation because it involves all 3 types of renormalization, and agreement between our answers and the well known results of Sommerfield and Petermann[17] would be confirmation that both the $P \to \infty$ limit and the renormalizations were correctly handled. We also hoped that our techniques would prove competitive with the Feynman approach, so that we could proceed to calculate part of the 6th order moment. We begin with the calculation of the second order anomalous moment.[18] Consider the graph shown in Figure 14, in which the external photon has x = 0 and polarization index 0. x and $\vec{k}$ are labeled for each line. By our rules the matrix element, without external fermion spinors is

$$\mathcal{M} = - \frac{e^2}{2(2\pi)^3} \int \frac{d^2x\, dx}{x(1-x)^2} \gamma^\mu (\not{p}_1 + m)\gamma^0(\not{p}_2+m)\gamma_\mu$$

$$\times \frac{1}{m^2 + \frac{\vec{q}_\perp^{\,2}}{4} - \frac{\vec{k}^2}{x} - \frac{(\vec{k} - \vec{q}/2)^2 + m^2}{1-x}} \quad \frac{1}{m^2 + \frac{\vec{q}_\perp^{\,2}}{4} - \frac{\vec{k}^2}{x} - \frac{(\vec{k} + \vec{q}/2)^2 + m^2}{1-x}} \tag{4.1}$$

where p_1, p_2 are on shell vectors with space components $\overrightarrow{(k+q/2,\ (1-x)P)}$, $\overrightarrow{(k-q/2,\ (1-x)P)}$.

It is readily verified that the anomalous moment is obtained from $\mathcal{M}$ by

$$F_2(0) = \lim_{q\to 0} \lim_{P\to\infty} \frac{2m^2}{4} \mathrm{Tr} \frac{\left\{\mathcal{M}(\not{p} - \frac{\not{q}}{2} + m)(\frac{\gamma^0}{P} - \frac{1}{m})(\not{p} + \frac{\not{q}}{2} + m)\right\}}{-q^2 P} \tag{4.2}$$

where p - q/2, p + q/2 are on shell vectors with space components $(-\vec{q}/2,\ P)$ and $(\vec{q}/2,\ P)$ respectively.

Performing the trace and taking the appropriate limits we obtain

$$F_2(0) = 2m^2 \frac{e^2}{(2\pi)^3} \int_0^1 dx\, x^2(1-x) \int d^2k \frac{1}{(\vec{k}^2 + m^2x^2)^2}$$

$$= 2m^2 \frac{e^2}{(2\pi)^3} \int_0^1 dx \frac{(1-x)}{m^2} \pi = \frac{\alpha}{2\pi} \tag{4.3}$$

In the lowest order calculations the x variable plays the role of the Feynman denominator-combining parameter. This identification, however, cannot be made in general.

There are five different Feynman graphs contributing to the magnetic moment in fourth order. They are shown together with the corresponding time ordered graphs in Figure 15. As explained in Section II, it is sufficient to consider only those time orderings with all $x_i > 0$.

We wrote a 2-stage program to perform these calculations. The first stage was a symbolic and algebraic program written in REDUCE.[19] It took as input the topology of the Feynman graph, and automatically generated the surviving time orders, set up and performed the required traces, computed the energy denominators and expressed everything in terms of the infinite momentum frame variables. The output is a set of Fortran expressions, which served as input to the second stage, a multidimensional integration program written by G. Sheppey.[20] The vacuum polarization graph was handled as indicated in the previous section. As independent variables for the crossed and corner graphs, we used x and $\vec{k}$ for each of the 2 virtual photons. In the ladder and self energy graphs, we parametrized the momenta of the photons by

1) Outer photon $\quad x = x_1$

$$\vec{k} = \vec{k}_1$$

2) Inner photon $\quad x = x_2(1-x_1)$

$$\vec{k} = \vec{k}_2 - x_2\vec{k}_1$$

With this choice, x_2 ranges between 0 and 1 and the energy denominators have no terms in $\vec{k}_1 \cdot \vec{k}_2$. This made the integrals over the directions of $\vec{k}_1$ and $\vec{k}_2$ trivial, so that the resulting integrals were four dimensional (over x_1, x_2, $\vec{k}_1^2$, $\vec{k}_2^2$), while those of the crossed and corner graphs were 5 dimensional.[21]

The crossed graph can be computed immediately,[22] since it requires no renormalization. The renormalization of the ladder and self-energy graphs were straightforward, as outlined in the previous section. The infrared piece of the ladder graph cancelled after symmetrizing the integrand in $(x_1, \vec{k}_1^2)$ and $(x_2, \vec{k}_2^2)$, while the infrared piece of the self-energy graph was removed as in the Feynman method.

The only difficult graph to renormalize was the corner graph. Until this point, our representation for the counter terms assured that the divergence (in the $\vec{k}$ integral) of the unrenormalized graph and the counter terms cancelled pointwise. In the corner graph, both IV(a) and IV(b) required subtraction. (See Fig. 16.) Although the divergence of both graphs adds up to that of the counter term, we did not find an elegant representation of the counter term $\frac{\alpha}{2\pi} \times L^{(2)}$ which renders each time order finite. What we did was to isolate the divergent pieces of each time order, and analytically computed the difference between these terms and the counter terms, using a regulator photon mass to assure covariance. Covariant regularization was essential in obtaining the right answer, since the subtraction of two divergent quantities is ambiguous. Our method in this graph was similar in spirit to intermediate renormalization[23] in standard QED calculations in which subtraction terms, differing from the usual counter terms, but with the same ultraviolet behavior, are introduced in intermediate stages of the calculation.

It should be noted that even for these graphs, our integrand was given by the infinite momentum frame rules. It was not necessary to renormalize at finite momentum and then take the infinite momentum limit.

To understand the origin of the difficulty in renormalizing the corner graph, recall that the photon incident on the reducible vertex piece has $x \neq 0$, whereas in the counter term, the photon is taken to have $q_\mu = 0$. Thus in the counter term, an insertion like cannot appear, since a photon with $x = 0$ cannot produce two fermions with positive x. Nevertheless, the main graph IV(b) containing this insertion diverges. The lines external to the reducible insertions in IV(b) do not satisfy energy conservation. Thus, the insertion is not Lorentz invariant, and it can be verified that graph IV(b) is finite in TOPTh in a frame with finite momentum. It is the limit $P \rightarrow \infty$ which gives rise to the divergence. This is of course possible, since the non-invariant insertion is frame dependent.

The results of our calculations agreed with the usual answers.[17] But as a pleasant surprise, it appeared that our integrands, expressed as a function of x_i and $\vec{k}_i$ are smoother than the corresponding usual integrands expressed as a function of the Feynman parameters. As a result, the numerical integrations (which are often the most difficult part of higher order calculations in QED) converge considerably faster. Typically, where comparisons could be made, the numerical integration time was between 2 and 5 times faster than the standard Feynman parameter method. This gain more than offsets the extra effort required to perform the infinite momentum frame algebra before integration.

These successes encouraged us to try some 6th order moment calculations. The results of this investigation for the Feynman graphs shown in Figure 17, have already been published.[24]

Meanwhile, diagram 17(a) has been computed analytically by Levine and Roskies.[25] Its value is [in units of $(\alpha/\pi)^3$]

$$\frac{g-2}{2} = \frac{733}{1728} + \frac{59\pi^2}{648} + \frac{7}{18}\zeta(3) = 1.7902778$$

to be compared with our estimate

$$1.777 \pm .013.$$

V. COVARIANT APPROACH AT $P = \infty$

Field theories at infinite momentum have been studied from a different point of view. Kogut and Soper[6] argued that the limit $P \rightarrow \infty$ is a reformulation of the theory in which the equal time surface (in the regular frame) is replaced by a light-like surface, i.e., $v = c$. Making the transformation

$$\tau = \frac{t+z}{\sqrt{2}}$$

$$z' = \frac{t-z}{\sqrt{2}}$$

they quantized the theory at equal τ. When passing from the Lagrangian to the Hamiltonian in this approach they found that the interaction Hamiltonian contained in addition to the usual piece a seagull term with the structure

$$e^2 \delta(\tau - \tau')\overline{\psi}\psi A_\mu A_\nu \quad .$$

that is, an instantaneous interaction involving 2 fermions and 2 photons. They then formulated TOPTh for this theory and reproduced the rules we have been discussing. In this approach the limit $P \rightarrow \infty$ never appears, it has already been taken. The question of whether this theory is equivalent to the usual one is the question of whether the $P \rightarrow \infty$ limit is justified. Their approach was formulated in the Coulomb gauge which is difficult to renormalize. Our results indicate that their rules are correct for renormalized amplitudes, and we have shown how to implement the renormalization procedure. A more covariant approach was developed by Chang, Root and Yan.[9] Starting with Schwinger's action principle, they "derived" the equal τ commutation relations which Kogut and Soper had guessed. They worked in the $\overline{\psi}\gamma^5\psi\phi$ theory rather than in QED. They found that the Feynman propagator was identical to the usual one for spin zero, but differed for spin 1/2. But they were able to show that the extra term in the spin 1/2 propagator exactly cancelled the terms arising from the seagull in the interaction Hamiltonian, so that their theory formally agreed with the usual one for renormalized amplitudes. Their expressions for the renormalization constants differed from the usual Feynman ones.

These results are easily understandable in terms of ours. Because the Feynman propagator only involves free fields, and because all free particles have $x > 0$, the fermion propagator does not include fermions with negative x. These must be contained in the effective interaction Hamiltonian, and they are exactly the seagull term. We have seen that fermions of negative x extend only over one time interval so that no other interaction can occur between its vertices. One can then effectively assume that its vertices are simultaneous. Formally one can also see this by noticing that the energy denominator associated with a state containing a particle of negative x is independent of the external energy, so that its Fourier transform is a delta function in time. Moreover, the seagull, a contracted z-graph, clearly involves 2 external fermions and 2 photons.

In a theory of scalar particles with no derivative coupling, our rules showed that at $P \to \infty$ there were no particles of negative x. Thus, the free propagator should agree with the Feynman result.

We can also understand why for example their expression for δm_e does not agree with ours. As a field theory, it was natural to interpret the seagull term as a normal ordered expression. But that means that it will not contribute to δm_e since its expectation value must be taken between states which have no photons. But we have seen that the seagull does contribute to the usual Feynman answer for δm_e, although its omission does not alter any renormalized amplitude.

Bouchiat et al.[8] have shown that if one does not normal order the seagull, the Feynman expression for δm_e is obtained.

CONCLUSIONS

We have demonstrated that TOPTh at infinite momentum is a viable practical calculational technique for higher order processes in QED. We have shown how to implement the renormalization procedure in a manner which closely parallels the usual method, and have demonstrated that for renormalized amplitudes the limit $P \to \infty$ may be taken before performing the phase space integrations, although this is not true in evaluating the renormalization constants themselves. Many of the concepts of the Feynman approach, such as off mass shell behavior, factorized vertices and self energy parts, and trace techniques, have a natural place in TOPTh_∞.

We have shown that our rules are equivalent to those obtained from quantizing on the light cone, but the study of the limit $P \to \infty$ allows us to extend that analysis to include a consistent renormalization program. Moreover, the discrepancy between the value of the renormalization constants evaluated in the light cone method and in the usual Feynman method is resolved. Our analysis puts field theoretic parton calculations on a rigorous basis, provided that a covariant regularization procedure is used.

Some of the advantages of TOPTh at infinite momentum are

1) Manifest unitarity, i.e., intermediate states have a definite number of on-mass-shell particles. This is sometimes more useful than manifest covariance. This is particularly true for bound state problems where one is dealing with wave functions.

2) The integrations over $\vec{k}^2$ and x in renormalized amplitudes are well behaved at the end points and are suitable for numerical evaluation.

3) Because of the close resemblance of this formulation with nonrelativistic theory, it is hoped that this approach will lead to a deeper understanding of field theory and to new approximation schemes for both QED and hadron physics. A procedure for calculating the bound state energies of positronium has already been developed by Feldman et al.[26] This method has been used to extend the impulse approximation to relativistic problems,[4] to calculate high energy Compton scattering,[27] and rearrangement collisions for relativistic systems.[28]

ACKNOWLEDGMENTS

It is a pleasure to acknowledge conversations with A. Casher, R. Goble, K. Johnson, D. Kershaw, M. Levine, J. Gunion, R. Blankenbecler, J. Bjorken and S. Drell.

One of us (R.R.) wishes to thank Yale University for the award of a Junior Faculty Fellowship for the academic year 1971-1972, thank S. Drell for the hospitality of the theoretical Physics Group at SLAC, where most of this work was performed, and to thank Y. Neeman for the hospitality of the physics department at Tel-Aviv University.

REFERENCES

1. S. Weinberg, Phys. Rev. 150, 1313 (1966). See also L. Susskind and G. Frye, Phys. Rev. 165, 1535 (1968); K. Bardakci and M. B. Halpern, Phys. Rev. 176, 1686 (1968).
2. S. Fubini and G. Furlan, Physics 1, 229 (1965); J. D. Bjorken, Phys. Rev. 179, 1547 (1969); R. Dashen and M. Gell-Mann, Phys. Rev. Letters 17, 340 (1966).
3. J. D. Bjorken and E. A. Paschos, Phys. Rev. 185, 1975 (1969), R. P. Feynman, see e.g. High Energy Collisions, edited by C. N. Yang et al., Gordon and Breach, New York (1969), p. 237.
4. S. D. Drell, D. J. Levy, and T. M. Yan, Phys. Rev. Letters 22, 744 (1969); Phys. Rev. 187, 2159 (1969); ibid D1, 1035, D1, 1617 (1970); S. D. Drell and T. M. Yan, Phys. Rev. D1, 2402 (1970); Phys. Rev. Letters 24, 181 (1970).
5. S. J. Chang and S. K. Ma, Phys. Rev. 180, 1506 (1969); ibid 188, 2385 (1969).
6. J. B. Kogut and D. E. Soper, Phys. Rev. D1, 2901 (1970); J. D. Bjorken, J. B. Kogut and D. E. Soper, Phys. Rev. D3, 1382 (1971).
7. R. Barbieri, J. A. Mignaco and E. Remiddi, Nuovo Cimento 11 A, 824, 865 (1972).
8. C. Bouchiat, P. Fayet and N. Sourlas, Lett. Nuovo Cimento 4, 9 (1972).
9. S. J. Chang, R. G. Root and T. M. Yan, Phys. Rev. D7, 1133 (1973). S. J. Chang and T. M. Yan, ibid, 1147 (1973), and University of Illinois preprints. J. H. Ten Eyck and F. Rohrlich, Syracuse University preprint, January 1973.
10. The sign convention is a consequence of the anticommutation property of the fermion field and guarantees Fermi statistics.

11. See the third paper of reference 4.

12. See Section IV.

13. The expression δm_a defined in (3.40) is still not well defined, and needs a further regularization. This can be done by writing

$$\delta m_a = \frac{e^2}{16\pi^3 m} \int d^2k \int_0^1 \frac{dx}{1-x} \int_0^\infty \rho(\lambda^2) \frac{m^2(2-2x-x^2) - \vec{k}^2}{\lambda^2(1-x) + \vec{k}^2 + m^2x^2}$$

where $\int \rho(\lambda^2) = 0$ and $\int \lambda^2 \rho(\lambda^2) = 0$. For ease of interpretation we retain the form written in the text.

14. It is possibly more convenient for radiative correction calculations to use a cutoff $s_\gamma = \vec{k}_\gamma^2/x_\gamma > s$ min, since this can be readily matched to the real photon phase-space integrations in the $P \to \infty$ frame.

15. S. Weinberg, Phys. Rev. 118, 838 (1960).

16. Recall that $V = 2B_i + B_e = F_i + F_e/2$.

17. C. M. Sommerfield, Phys. Rev. 107, 328 (1957); Ann. Phys. (N.Y.) 5, 26 (1958). A. Petermann, Helv. Phys. Acta 30, 407 (1957); Nucl. Phys. 3, 689 (1957).

18. D. Foerster, University of Sussex thesis (1973). Foerster's derivation of the lowest order anomalous moment $\alpha/2\pi$ is particularly instructive. If the electron interacts with a magnetic field (transverse photon polarization), then one finds that the contribution of Figure 2(a) without the z graph modification is negative (but logarithmic divergent) in agreement with Welton's classical argument (T. Welton, Phys. Rev. 74, 1157 (1948)). The surviving z-graph contributions of Figure 2(a) (and its mirror graph) are positive, canceling the divergent term, and leaving the finite $\alpha/2\pi$ remainder. Note that the z graph piece contains the Thomson limit part of the Compton

amplitude for the side-wise dispersion calculation of S. Drell and H. Pagels, Phys. Rev. 140B, 397 (1965). The remaining diagrams in Figure 2 vanish in the infinite momentum frame.

19. A. C. Hearn, Stanford University preprint No. ITP-247 (unpublished); and A. C. Hearn in: Interactive Systems for Experimental Applied Mathematics, eds. M. Klerer and J. Reinfields (Academic Press, New York, 1968).

20. See J. Aldins, S. Brodsky, A. Dufner, and T. Kinoshita, Phys. Rev. D1, 2378 (1970); A. Dufner, Proceedings of the Colloquium on Computation Methods in Theoretical Physics (Marseille, 1970) and B. Lautrup, Proceedings of the 2nd Colloquium on Computational Methods in Theoretical Physics, (Marseille, 1971).

21. In general a graph with n loops requires a maximum of (3n-1) integrations, as opposed to the Feynman parameter approach requiring (3n-2). Symmetries of graphs reduce the dimensionalities by the same number in both approaches.

22. For numerical integrations we used the transformation $\vec{k}_i^2 = x_i^2 \left(\frac{1}{z_i} - 1\right)$ $0 \leq z_i \leq 1$. This makes the range of all variables finite. This particular transformation also trivializes the second order moment calculation and we hoped it would smooth the higher order integrals.

23. See for example, S. J. Brodsky and J. D. Sullivan, Phys. Rev. 156, 1644 (1967).

24. S. Brodsky and R. Roskies, Phys. Lett. 41B, 517 (1972).

25. M. Levine and R. Roskies, Phys. Rev. Lett. 30, 772 (1973).

26. G. Feldman, T. Fulton and J. Townsend, John Hopkins University preprint (1972).

27. S. Brodsky, F. Close, and J. Gunion, Phys. Rev. D5, 1384 (1972).

28. J. Gunion, S. Brodsky, and R. Blankenbecler, Report No. SLAC-PUB-1053 and Phys. Letters 39B, 649 (1972).

29. M. Schmidt, Report No. SLAC-PUB-1265. See also S. Brodsky, F. Close and J. Gunion, SLAC-PUB-1243.

30. A similar result has been obtained independently by T. Yan, Phys. Rev. D7, 1781 (1973).

31. We wish to thank J. Kogut and D. Soper for a discussion on this point.

APPENDIX A

The Connection Between Feynman and Infinite Momentum Rules

In the appendix we give a simple connection between the Feynman rules and TOPTh in the infinite momentum frame for some low order graphs. This discussion extends the work of Chang and Ma[5] and Schmidt.[29]

Consider, as a first example, the calculation of the lowest QED vertex labeled as in Fig. 10. We retain the kinematics of Section IV. The Feynman rules give

$$M_\nu = \int \frac{d^4k/i}{(2\pi)^4} \quad \frac{\gamma^\mu(\not{p}_1 + m)\gamma_\nu(\not{p}_2 + m)\gamma_\mu}{(p_1^2 - m^2 + i\epsilon)(p_2^2 - m^2 + i\epsilon)(k^2 - \lambda^2 + i\epsilon)} \tag{A-1}$$

We parameterize the four-momenta as follows $(\vec{q}^{\,2} = -q^2)$

$$\begin{aligned} q &= (0, \vec{q}, 0) \\ p &= \left(P + \frac{m^2 + \vec{q}^{\,2}/4}{4P}, \vec{0}, P - \frac{m^2 + \vec{q}^{\,2}/4}{4P}\right) \\ k &= \left(xP + \frac{k^2 + \vec{k}^2}{4xP}, \vec{k}, xP - \frac{k^2 + \vec{k}^2}{4xP}\right) \end{aligned} \tag{A-2}$$

Notice that the mass-shell conditions for $p \pm q/2$, q and k are satisfied independent of the value of P. Thus P is an arbitrary parameter of the frame choice; $y = \log 2P/m$ is the rapidity of the incident electron. Of course, in the frame where $P \to \infty$, the quantity $x \equiv (k_0 - k_3)/2P$ is the fractional longitudinal momentum carried by the photon.

The four degrees of freedom of k^2 are replaced by x, $\vec{k}$, and k^2

$$d^4k = d^2k \quad \frac{dx}{2\,|x|} \quad dk^2 \tag{A-3}$$

Assuming uniform convergence, the k^2 integration may be performed immediately from the pole structure of the integrand of (A-1).

$$p_1^2 - m^2 + i\epsilon = (p + q/2 - k)^2 - m^2 + i\epsilon$$

$$= (1-x)\left[m^2 + \vec{q}^{\,2}/4 - \frac{(\vec{k})^2 + k^2}{x} - \frac{(\vec{k} - \vec{q}/2)^2 + m^2}{1-x}\right] + i\epsilon$$

$$p_2^2 - m^2 + i\epsilon = (p - q/2 - k)^2 - m^2 + i\epsilon \tag{A-4}$$

$$= (1-x)\left[m^2 + \vec{q}^{\,2}/4 - \frac{(\vec{k})^2 + k^2}{x} - \frac{(\vec{k} + \vec{q}/2)^2 + m^2}{1-x}\right] + i\epsilon$$

The k^2 integration clearly is zero unless $0 \leq x \leq 1$. Closing the contour below, we pick-up the $k^2 = \lambda^2 - i\epsilon$ pole and obtain

$$M_\nu = -\int d^2k \int_0^1 \frac{dx}{2x(1-x)^2} \frac{\gamma^\mu(\not{p}_1+m)\gamma_\nu(\not{p}_2+m)\gamma_\mu\Big|_{k^2=\lambda^2}}{\left[m^2 - \frac{(\vec{k}+x\vec{q}/2)^2+\lambda^2}{x} - \frac{(\vec{k}+x\vec{q}/2)^2+m^2}{1-x}\right]}$$

$$\times \left[m^2 - \frac{(\vec{k}-x\vec{q}/2)^2+\lambda^2}{x} - \frac{(\vec{k}-x\vec{q}/2)^2+m^2}{1-x}\right] \tag{A-5}$$

which is exactly the infinite momentum TOPTh result. Notice that p_1^μ and p_2^μ in the numerator are computed from energy conservation using the on-mass shell calculation for the photon

$$p_1 \to (p-q/2)-k\Big|_{k^2=\lambda^2} = \left[(1-x)P + \frac{m^2+\frac{1}{4}\vec{q}^{\,2}}{4P} - \frac{\lambda^2+\vec{k}^2}{4xP},\ -\vec{k} - \frac{\vec{q}}{2},\right.$$

$$\left.(1-x)P - \frac{m^2+\frac{1}{4}\vec{q}^{\,2}}{4P} + \frac{\lambda^2+\vec{k}^2}{4xP}\right] \tag{A-6}$$

This coincides with the rule for automatic z-graph inclusion given in Section II. Equation (A-5) is valid for any component of M_ν, assuming regulatization in the photon mass.

Let us also consider a two-loop example, the crossed-graph contribution to the electron vertex (see Fig. 15, II). We again parametrize the loop momentum as in Eq. (A-2) with

$$k^\mu_{(i)} = \left(x_i P + \frac{k_i^2 + \vec{k}^2}{4x_i P}\ ,\ \vec{k}_i,\ x_i P - \frac{k_i^2 + \vec{k}^2}{4x_i P} \right) \tag{A-7}$$

The poles in k_i^2 derive from the photon propagators and

$$(p - q/2 - k_1)^2 - m^2 + i\epsilon \sim -(1-x_1)\,\frac{k_1^2}{x_1} + i\epsilon + \ldots$$

$$(p + q/2 - k_2)^2 - m^2 + i\epsilon \sim -(1-x_2)\,\frac{k_2^2}{x_2} + i\epsilon + \ldots \tag{A-8}$$

$$(p \pm q/2 - k_1 - k_2)^2 - m^2 + i\epsilon \sim -(1-x_1-x_2)\left[\frac{k_1^2}{x_1} + \frac{k_2^2}{x_2}\right] + i\epsilon \ldots$$

For $1-x_1-x_2 > 0$, we close the contours below, pick up contributions from $k_1^2 = \lambda^2 - i\epsilon$, $k_2^2 = \lambda^2 - i\epsilon$, and obtain a result identical to that of the infinite momentum frame for Fig. 15, II, a. The lepton energies are obtained from energy conservation from the initial state particles and the on-shell photons. However, for $1-x_1-x_2 < 0$, we close the k_1^2 and k_2^2 contours above, and pick up contributions from

$$(p + q/2 - k_2)^2 = m^2 - i\epsilon \qquad \text{and} \qquad (p - q/2 - k_1)^2 = m^2 - i\epsilon, \tag{A-9}$$

and obtain the infinite momentum result for Fig. 15, II, b. In this case the energy of the lepton lines $p + q/2 - k_2$ and $p - q/2 - k_1$ (which cross two-time intervals) is obtained from the on-shell condition. For the other lepton lines, we use energy conservation between the initial and intermediate state

$$k_1 + k_2 - p + q/2 = q + (p - q/2) - (p - q/2 - k_1) - (p + q/2 - k_2) \qquad \text{(A-10)}$$

to determine the correct energy values. These results again agree with the automatic z-graph rule given in Section II.

It is of course obvious from this explicitly-covariant approach that the same basic Dirac algebra or trace occurs independent of the time-ordering and it is identical to the Feynman result.

One important caution in carrying out this procedure is that the resulting $d^2k\, dx$ integration must be finite after the k^2 integration is performed; otherwise the lack of uniform convergence can be reflected by extra δ-function contributions, which reflect surviving contributions from non-forward graphs in the $P \to \infty$ TOPTh calculations.

As an example of the occurrence of an essential $\delta(x)$ contribution, let us return to the δm calculation of Section III-F. The Feynman result is

$$\bar{u}u\delta m = \frac{e^2}{(2\pi)^4} \int d^4k/i \int \rho(\lambda^2)d\lambda^2 \frac{\bar{u}(p)\gamma_\mu(\not{p} - \not{k} + m)\gamma^\mu u(p)}{(k^2-\lambda^2+i\epsilon)\left((p-k)^2 - m^2 + i\epsilon\right)} \qquad \text{(A-11)}$$

or

$$m\delta m = \frac{e^2}{(2\pi)^4} \int d^2k \int \frac{dx}{2|x|} \int \frac{dk^2}{i} \int \frac{\rho(\lambda^2)d\lambda^2\, [2m^2 + 2p\cdot k]}{(k^2-\lambda^2+i\epsilon)\left((p-k)^2 - m^2 + i\epsilon\right)}$$

(A-12)

Here we covariantly regularize in the photon mass by setting the zeroth and first moment of the spectral function $\rho(\lambda^2)$ to zero. As always the λ^2 integration is to be performed first.

The numerator can be written in the form

$$4m^2 - 2p \circ (p-k) = 3m^2 + xm^2 - \frac{\vec{k}^2 + m^2}{1-x} - \frac{(p-k)^2 - m^2}{1-x} \qquad \text{(A-13)}$$

The first three terms correspond to δm_a of Section III, and gives Eq. (3.40) after the k^2 integration is performed. For the last term we note the distribution identity[30]

$$\frac{1}{2\ x} \int \frac{dk^2}{i} \int \frac{\rho(\lambda^2) d\lambda^2}{k^2 - \lambda^2 - i\epsilon} = \frac{-\pi}{2}\ \delta(x) \int \rho(\lambda^2) d\lambda^2 \log(\vec{k}^2 + \lambda^2) \qquad \text{(A-14)}$$

This follows from the fact that the left side of (A-14) vanishes for $x \neq 0$, and

$$\int d^4k/i \int \frac{\rho(\lambda^2) d\lambda^2}{k^2 - \lambda^2 + i\epsilon} = \frac{-\pi}{2} \int d^2k \int \rho(\lambda^2) d\lambda^2 \log (\vec{k}^2 + \lambda^2) \qquad \text{(A-15)}$$

which is the usual result obtained from doing the k_0 and k_3 integrations.

Thus the origin of the δm_b term Eq. (3.41), which corresponds to the singular $x \sim 0$ contribution of the backward graph in the $P \to \infty$ TOPTh calculation, is the singular nature of the transformation (A-3) in the k^2-integration method. Note that the explicit occurrence of the δm_b contribution can be formally avoided if one uses (the unconventional) regularization in both the internal photon and lepton mass.[31]

The extra δ-function terms can always be avoided if covariant regularization of the photon and lepton propagators is assumed, and thus never occur in our QED calculations of regularized or renormalized amplitudes. In the vacuum polarization calculation, regularization in the mass of the loop fermion must be used. In the vertex calculations, photon regularization is sufficient.

Unfortunately, this prescription of performing the k^2 integral does not always generate the TOPTh_∞ integrands. This is perhaps most easily seen in tree graphs, which require no integrations. One can easily see that the

Feynman amplitude is then a <u>sum</u> of different $TOPTh_\infty$ graphs, and no simple operation on individual propagators can reproduce the separate time ordered integrands, because the number of surviving time orders is not always of the form $(\text{constant})^n$, where n is the number of internal propagators.

FIGURE CAPTIONS

1. Feynman vertex graph in third order.

2. The six time-ordered contributions to the Feynman vertex graph of figure 1. By convention, time flows from left to right.

3. Time-ordered contribution to the self-energy containing a backward moving fermion.

4. Feynman graph for a self-energy insertion in the Compton amplitude.

5. (a) Vacuum polarization contribution to particle scattering.

   (b) Vacuum polarization insertion calculated in eq. (3.19).

6. Time-ordered contributions corresponding to the vacuum polarization insertion in a vertex correction to electron-electron scattering. The three time-orders combine, when renormalized, to the renormalized covariant photon propagator modification for figure 7.

7. Vertex correction to electron-electron scattering.

8. Contribution to electron-electron scattering from time-ordered perturbation theory.

9. General vertex correction to electron-electron scattering. When all internal time-ordered contributions are combined, the covariant vertex correction (3.24) results.

10. Labeling of the two-photon ladder graph contribution to the electron vertex.

11. Time-ordered contribution to the electron self-energy. Because of the Pauli principle (c) contributes instead of (b) when $p' = p$.

12. Time-ordered contributions for a self-energy correction to the electron vertex.

13. Mass shift subtraction terms for the two time-ordered self-energy contributions of figure (12), corresponding to eqs. (3.40) and (3.41) respectively.

14. Labeling of the vertex diagram for the anomalous moment calculation.

15. Contributions to the order α^2 corrections to the electron vertex. The left column shows the Feynman graph. The other columns display the corresponding essential time-ordered contributions as $P \to \infty$.

16. Vertex insertion for the Feynman "corner" graph of figure 15.

17. Feynman graph contributions to the sixth order magnetic moment computed using time-ordered perturbation theory techniques.

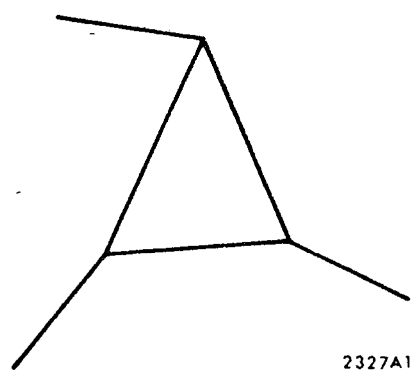

2327A1

FIG. 1

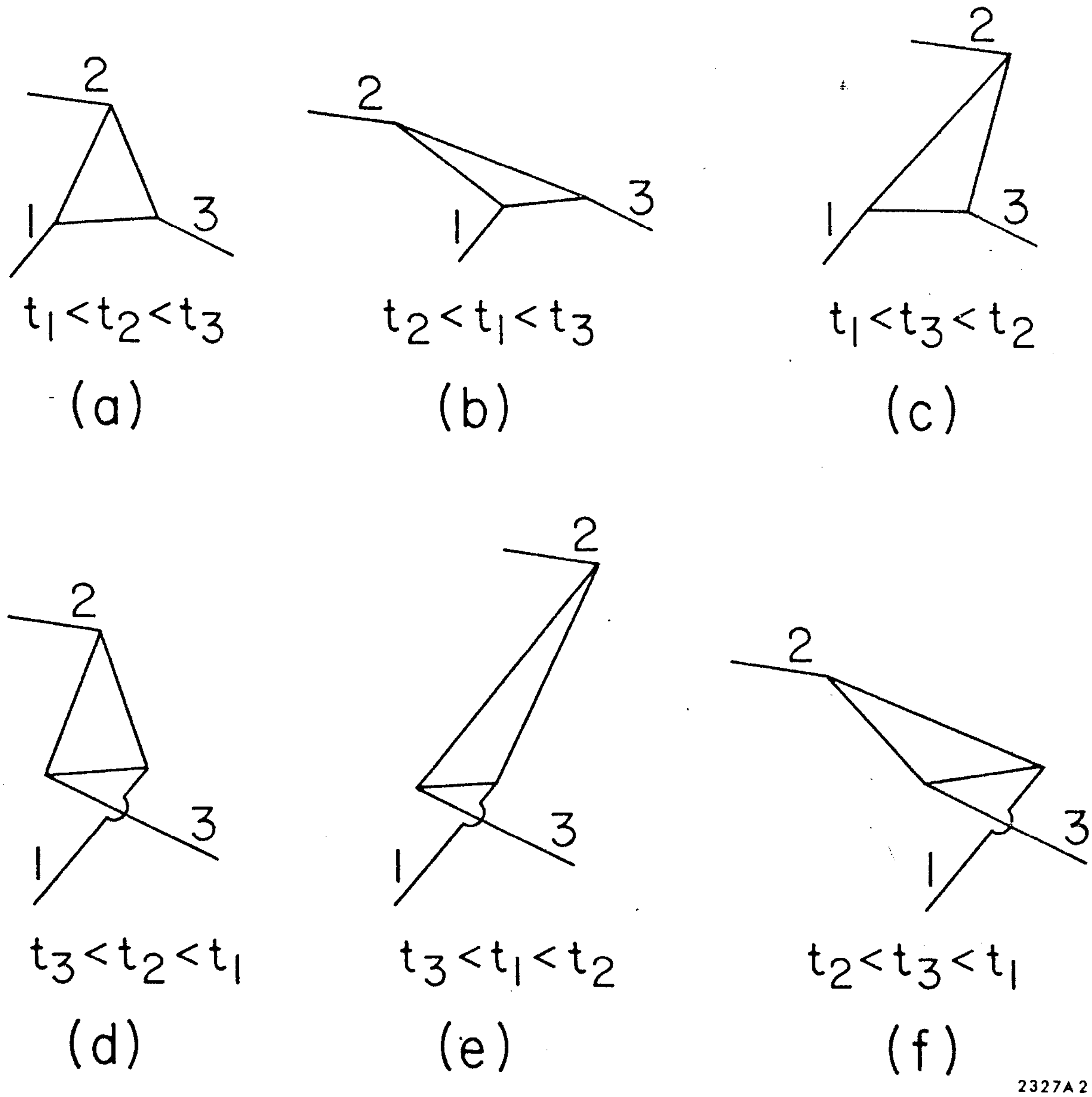

2
1
3
$t_1 < t_2 < t_3$
(a)
2
3
1
$t_2 < t_1 < t_3$
(b)
2
1
3
$t_1 < t_3 < t_2$
(c)
2
3
1
$t_3 < t_2 < t_1$
(d)
2
3
1
$t_3 < t_1 < t_2$
(e)
2
3
1
$t_2 < t_3 < t_1$
(f)
2327A2

FIG. 2

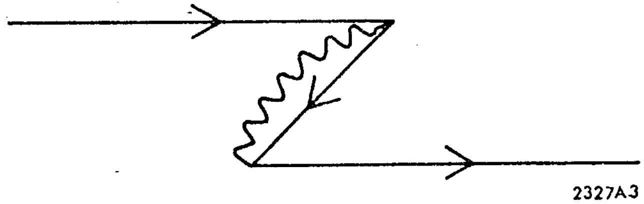

FIG. 3

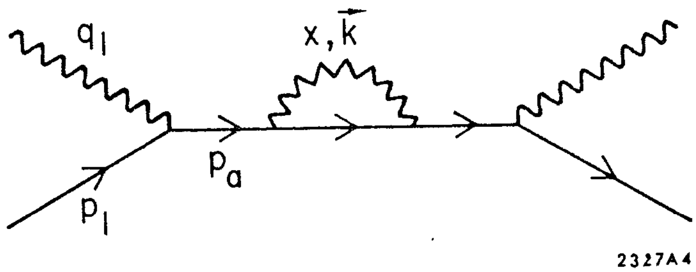

FIG. 4

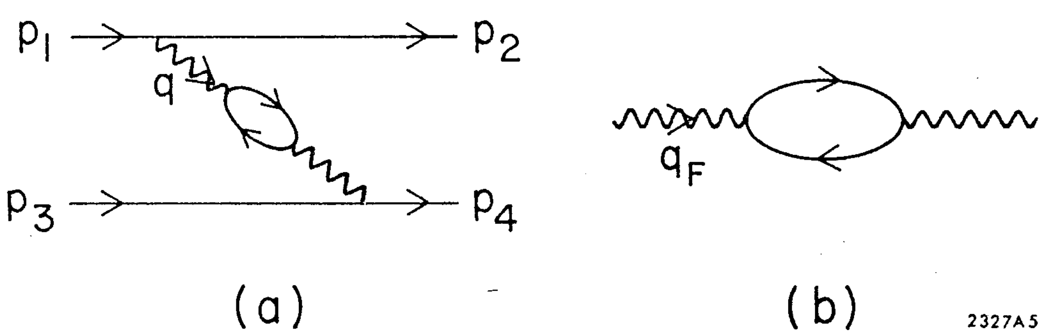

FIG. 5

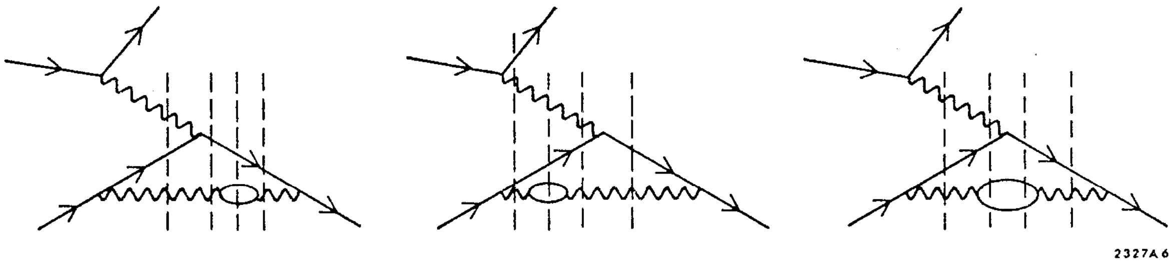

FIG. 6

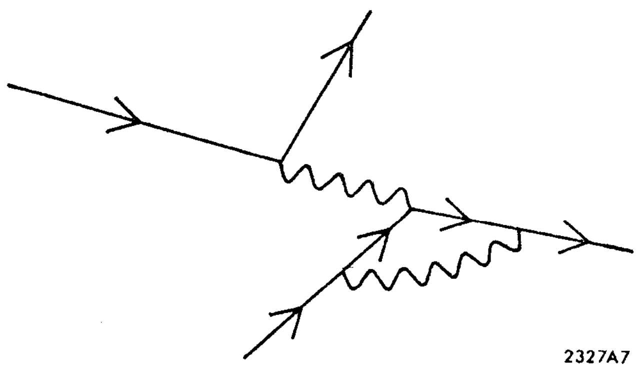

FIG. 7

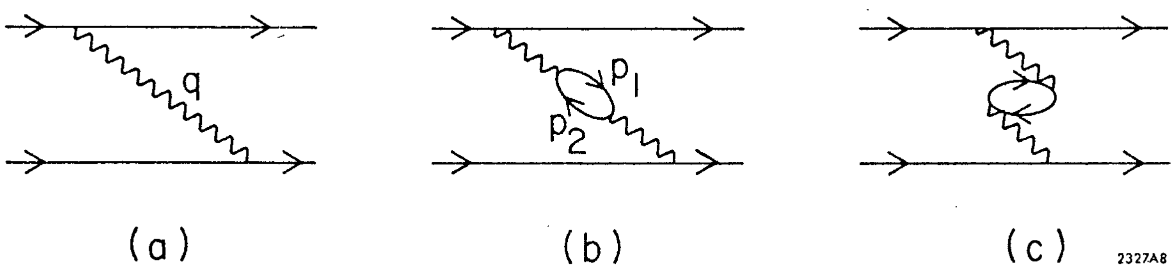

FIG. 8

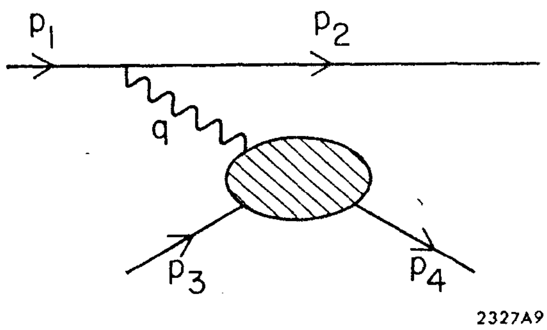

FIG. 9

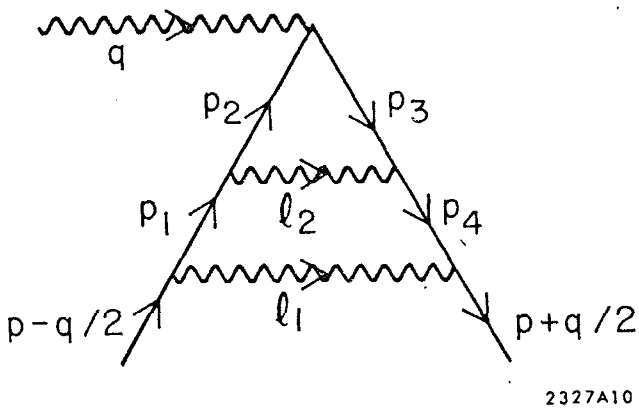

FIG. 10

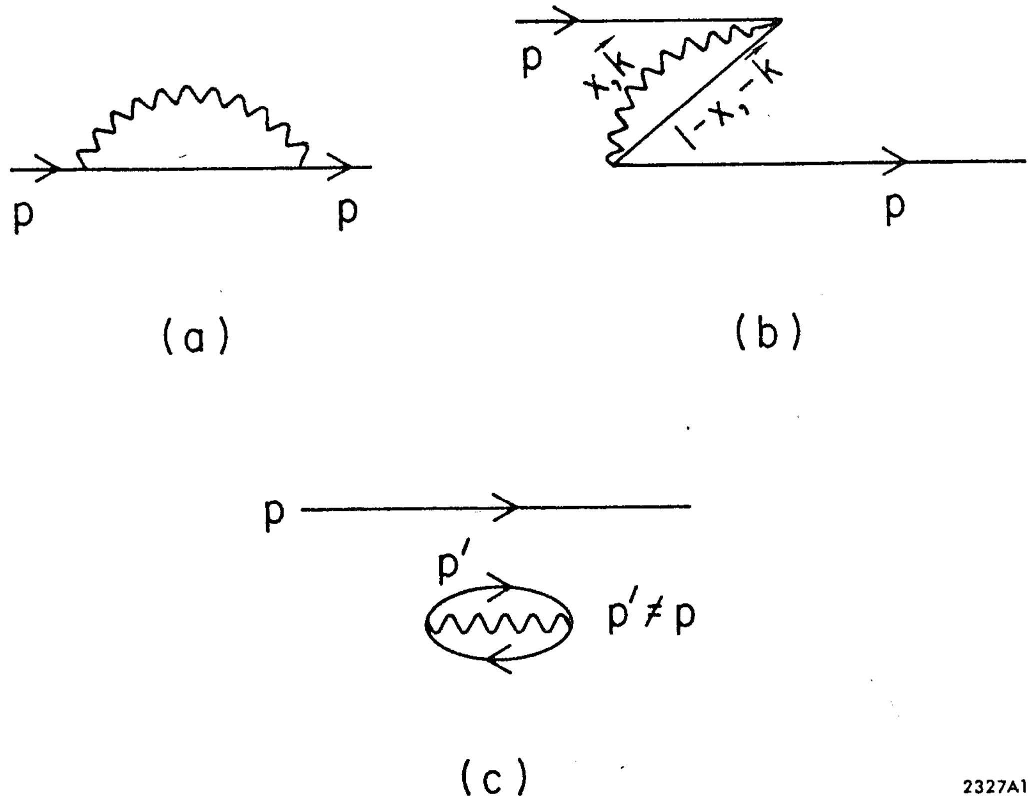

FIG. 11

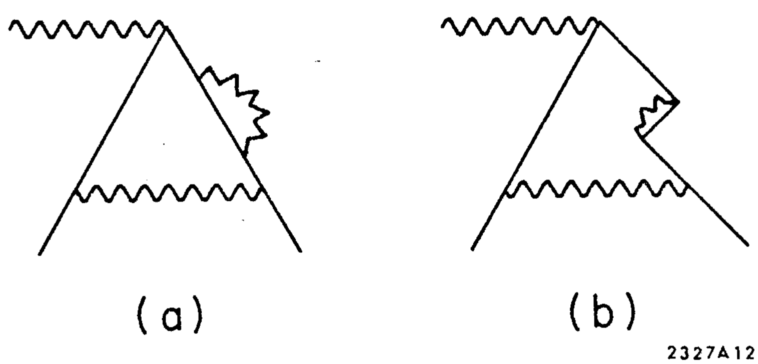

FIG. 12

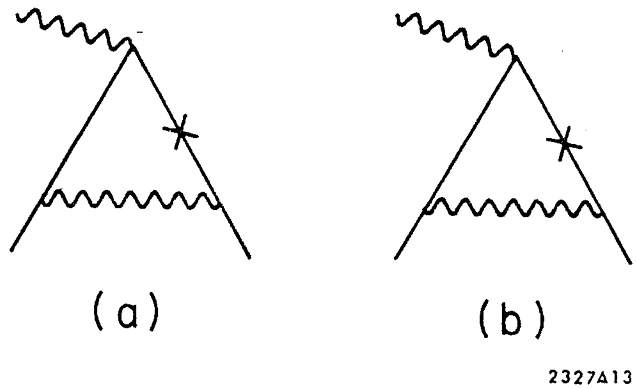
(a)
(b)
2327A13

FIG. 13

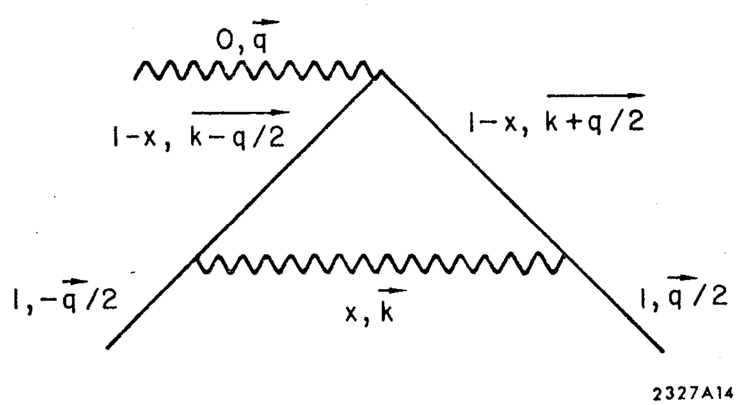
0, $\vec{q}$
1-x, $\overrightarrow{k-q/2}$
1-x, $\overrightarrow{k+q/2}$
1, $-\vec{q}/2$
x, $\vec{k}$
1, $\vec{q}/2$
2327A14

FIG. 14

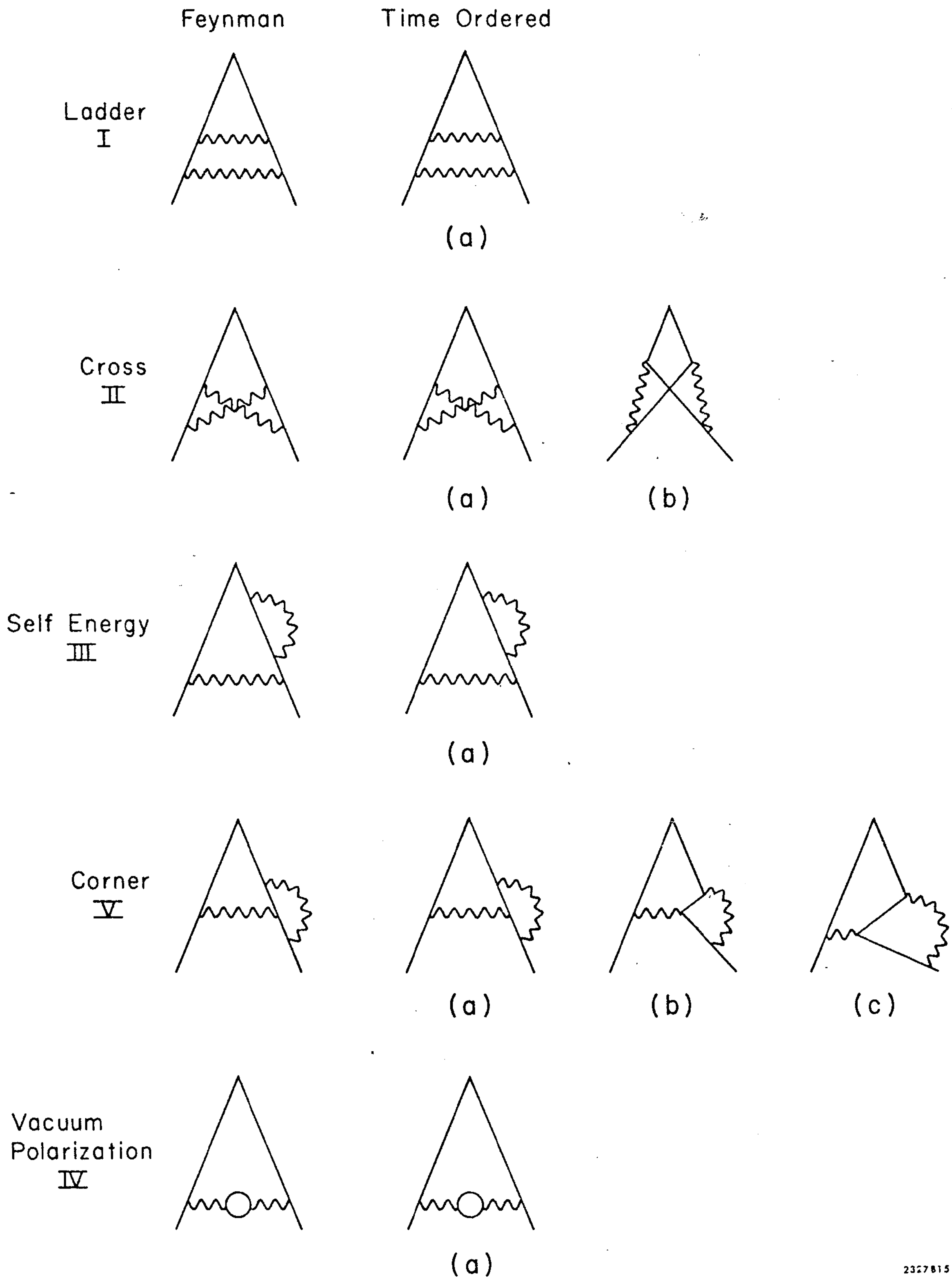

Feynman
Time Ordered
Ladder
I
(a)
Cross
II
(a)
(b)
Self Energy
III
(a)
Corner
V
(a)
(b)
(c)
Vacuum
Polarization
IV
(a)
2327815

FIG. 15

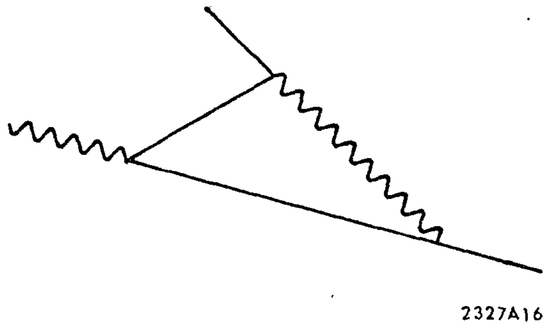

FIG. 16

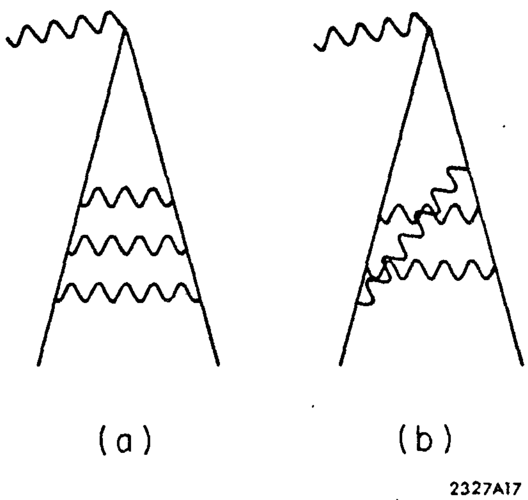

FIG. 17